ORTA DOĞU TEKNİK ÜNİVERSİTESİ
FEN BİLİMLERİ ENSTİTÜSÜ MÜDÜRLÜĞÜ

TEZ ŞABLONU ONAY FORMU
THESIS TEMPLATE CONFIRMATION FORM

1. Şablonda verilen yerleşim ve boşluklar değiştirilmemelidir.

2. **Jüri tarihi** Başlık Sayfası, İmza Sayfası, Abstract ve Öz'de ilgili yerlere yazılmalıdır.

3. İmza sayfasında jüri üyelerinin unvanları doğru olarak yazılmalıdır. Tüm imzalar **mavi pilot kalemle** atılmalıdır.

4. **Disiplinlerarası** programlarda görevlendirilen öğretim üyeleri için jüri üyeleri kısmında tam zamanlı olarak çalıştıkları anabilim dalı başkanlığının ismi yazılmalıdır. Örneğin: bir öğretim üyesi Biyoteknoloji programında görev yapıyor ve biyoloji bölümünde tam zamanlı çalışıyorsa, İmza sayfasına biyoloji bölümü yazılmalıdır. İstisnai olarak, disiplinler arası program başkanı ve tez danışmanı için disiplinlerarası program adı yazılmalıdır.

5. Tezin **son sayfasının sayfa** numarası Abstract ve Öz'de ilgili yerlere yazılmalıdır.

6. Bütün chapterlar, referanslar, ekler ve CV sağ sayfada başlamalıdır. Bunun için **kesmeler** kullanılmıştır. **Kesmelerin kayması** fazladan boş sayfaların oluşmasına sebep olabilir. Bu gibi durumlarda paragraf (¶) işaretine tıklayarak kesmeleri görünür hale getirin ve yerlerini **kontrol edin**.

7. Figürler ve tablolar kenar boşluklarına taşmamalıdır.

8. Şablonda yorum olarak eklenen uyarılar dikkatle okunmalı ve uygulanmalıdır.

9. Tez yazdırılmadan önce PDF olarak kaydedilmelidir. Şablonda yorum olarak eklenen uyarılar PDF dokümanında yer almamalıdır.

10. Tez taslaklarının kontrol işlemleri tamamlandığında, bu durum öğrencilere METU uzantılı öğrenci e-posta adresleri aracılığıyla duyurulacaktır.

11. Tez yazım süreci ile ilgili herhangi bir sıkıntı yaşarsanız, [Sıkça Sorulan Sorular (SSS)](#) sayfamızı ziyaret ederek yaşadığınız sıkıntıyla ilgili bir çözüm bulabilirsiniz.

---

1. Do not change the spacing and placement in the template.

2. Write **defense date** to the related places given on Title page, Approval page, Abstract and Öz.

3. Write the titles of the examining committee members correctly on Approval Page. **Blue ink** must be used for all signatures.

4. For faculty members working in **interdisciplinary programs**, the name of the department that they work full-time should be written on the Approval page. For example, if a faculty member staffs in the biotechnology program and works full-time in the biology department, the department of biology should be written on the approval page. Exceptionally, for the interdisciplinary program chair and your thesis supervisor, the interdisciplinary program name should be written.

5. Write **the page number of the last page** in the related places given on Abstract and Öz pages.

6. All chapters, references, appendices and CV must be started on the right page. **Section Breaks** were used for this. **Change in the placement** of section breaks can result in extra blank pages. In such cases, make the section breaks visible by clicking paragraph (¶) mark and **check their position.**

7. All figures and tables must be given inside the page. Nothing must appear in the margins.

8. All the warnings given on the comments section through the thesis template must be read and applied.

9. Save your thesis as pdf and Disable all the comments before taking the printout.

10. This will be announced to the students via their METU students e-mail addresses when the control of the thesis drafts has been completed.

11. If you have any problems with the thesis writing process, you may visit our [**Frequently Asked Questions (FAQ)**](#) page and find a solution to your problem.

☒ **Yukarıda bulunan tüm maddeleri okudum, anladım ve kabul ediyorum. / I have read, understand and accept all of the items above.**

Name : Yalçın
Surname : Boztaş
E-Mail : e166648@metu.edu.tr
Date : 11.05.2022
Signature : _____

SYNTHESIS AND POLYMERIZATION OF NEW D-A-D TYPE MONOMERS
BEARING FLUORINATED BENZOTHIADIAZOLE ACCEPTORS AND
THEIR OPTOELECTRONIC APPLICATIONS

A THESIS SUBMITTED TO
THE GRADUATE SCHOOL OF NATURAL AND APPLIED SCIENCES
OF
MIDDLE EAST TECHNICAL UNIVERSITY

BY

YALÇIN BOZTAŞ

IN PARTIAL FULFILLMENT OF THE REQUIREMENTS
FOR
THE DEGREE OF MASTER OF SCIENCE
IN
CHEMISTRY

MAY 2022

Approval of the thesis:

SYNTHESIS AND POLYMERIZATION OF NEW D-A-D TYPE MONOMERS BEARING FLUORINATED BENZOTHIADIAZOLE ACCEPTORS AND THEIR OPTOELECTRONIC APPLICATIONS

submitted by **YALÇIN BOZTAŞ** in partial fulfillment of the requirements for the degree of **Master of Science** in **Chemistry, Middle East Technical University** by,

Prof. Dr. Halil Kalıpçılar
Dean, Graduate School of **Natural and Applied Sciences**　　　_____

Prof. Dr. Özdemir Doğan
Head of the Department, **Chemistry**　　　_____

Prof. Dr. Ahmet M. Önal
Supervisor, **Chemistry, METU**　　　_____

Examining Committee Members:

Prof. Dr. Ali Çırpan
Chemistry, METU　　　_____

Prof. Dr. Ahmet M. Önal
Chemistry, METU　　　_____

Prof. Dr. Atilla Cihaner
Chemical Eng., Atılım Uni.　　　_____

Assoc. Prof. Dr. Merve İçli Özkut
Chemical Eng., Ankara Uni.　　　_____

Dr. Hasan Tarık Baytekin
Chemistry, METU　　　_____

Date: 11.05.2022

I hereby declare that all information in this document has been obtained and presented in accordance with academic rules and ethical conduct. I also declare that, as required by these rules and conduct, I have fully cited and referenced all material and results that are not original to this work.

Name Last name : Yalçın Boztaş

Signature :

ABSTRACT

SYNTHESIS AND POLYMERIZATION OF NEW D-A-D TYPE MONOMERS BEARING FLUORINATED BENZOTHIADIAZOLE ACCEPTORS AND THEIR OPTOELECTRONIC APPLICATIONS

Boztaş, Yalçın
Master of Science, Chemistry
Supervisor : Prof. Dr. Ahmet M. Önal

May 2022, 47 pages

In this study, a new series of alkylenedioxythiophene (ProDOT) type monomers bearing substituted and unsubstituted benzothiadiazole acceptor units was synthesized, and the resulting derivatives were characterized by using NMR spectroscopy, elemental analysis and HRMS techniques. The monomers were polymerized by electrochemical polymerization method. The electrochemical and optical properties of monomers and their corresponding polymers were thoroughly investigated in detail to elucidate how the number of fluorine atoms in the benzothiadiazole acceptor unit affects them. For the electrochemical investigations both differential pulse and cyclic voltammetry methods were used. In addition, the spectroelectrochemical properties of newly synthesized polymers were investigated.

Keywords: Fluorinated Benzothiadiazole, ProDOT, Donor-Acceptor-Donor, Electrochromic Polymers

ÖZ

FLOR SÜBSTİTÜE EDİLMİŞ BENZOTİYADİAZOL ALICI GRUBU İÇEREN YENİ V-A-V (VERİCİ-ALICI-VERİCİ) TİPİ MONOMERLERİN SENTEZİ, POLİMERİZASYONU VE OPTOELEKTRONİK UYGULAMALARI

Boztaş, Yalçın
Yüksek Lisans, Kimya
Tez Yöneticisi: Prof. Dr. Ahmet M. Önal

Mayıs 2022, 47 sayfa

Bu çalışmada, flor sübstitüe edilmiş ve edilmemiş benzotiyadiazol alıcı grubu içeren yeni alkilendioksitiyofen (ProDOT) tipindeki monomerler sentezlendi ve elde edilen monomerler NMR, elemental analiz ve HRMS teknikleri kullanılarak karakterize edildi. Sonrasında, elde edilen monomerler elektrokimyasal yöntemlerle polimerleştirildi. Benzotiyadiazol alıcı grubundaki farklı sayıdaki flor atomunun monomer ve polimerlerin elektrokimyasal ve optik özelliklerine etkileri detaylı olarak incelendi. Elektrokimyasal çalışmalarda döngüsel voltametri ve diferansiyel puls voltametri teknikleri kullanıldı. Ayrıca, sentezlenmiş yeni polimerlerin spektroelektrokimyasal özellikleri de incelendi.

Anahtar Kelimeler: Benzotiyadiazol, ProDOT, Verici-Alıcı-Verici, Elektrokromik Polimerler

To my beloved family…

ACKNOWLEDGMENTS

I would like to express my deepest gratitude to Prof. Dr. Ahmet M. Önal for his endless support and wisdom. I will always be honored for being a graduate as his student.

I would like to thank Dr. Deniz Çakal for her guidance, advises and infinite encouragements.

I would like to thank my family for their support and love.

I would like to thank my laboratory mates Deniz Eroğlu, Samet Şanlı, Elif Demir Arabacı and Merve Akbayrak for their precious friendship.

Special thanks to Güzide Aykent for not only being in my life but also for being my life. I feel incredibly blessed with her presence in my life.

TABLE OF CONTENTS

x

LIST OF TABLES

TABLES

LIST OF SCHEMES

SCHEMES

LIST OF FIGURES

FIGURES

LIST OF ABBREVIATIONS

ABBREVIATIONS

P0	4,7-bis(3,3-didecyl-3,4-dihydro-2H-thieno[3,4-b][1,4]dioxepin-6-yl)benzo[c][1,2,5]thiadiazole
P1	4,7-bis(3,3-didecyl-3,4-dihydro-2H-thieno[3,4-b][1,4]dioxepin-6-yl)-5-fluorobenzo[c][1,2,5]thiadiazole
P2	4,7-bis(3,3-didecyl-3,4-dihydro-2H-thieno[3,4-b][1,4]dioxepin-6-yl)-5,6-difluorobenzo[c][1,2,5]thiadiazole
E_g	Band Gap Energy
D-A-D	Donor-Acceptor-Donor
D	Electron Donating
A	Electron Withdrawing
BTD	2,1,3-Benzothiadiazole
EDOT	Ethylenedioxythiophene
ProDOT	Propylenedioxythiophene
HOMO	Highest Occupied Molecular Orbital
LUMO	Lowest Unoccupied Molecular Orbital
VB	Valence Band
CB	Conduction Band
NMR	Nuclear Magnetic Resonance
HRMS	High Resolution Mass Spectrometry
CV	Cyclic Voltammetry

DPV	Differential Pulse Voltammetry
ICT	Intramolecular Charge Transfer
ACN	Acetonitrile
DCM	Dichloromethane
THF	Tetrahydrofuran
TBAPF$_6$	Tetrabutylammonium hexafluorophosphate
t$_s$	Switching Time
CE	Coloration Efficiency

CHAPTER 1

INTRODUCTION

Although there was no knowledge of polymers or macromolecules among people prior to the 1920s, polymers have always found a place in human life throughout history, beginning with natural polymers such as cotton, wool, silk, and so on. In the 1920s, Hermann Staudinger proposed a ground-breaking chain theory, and he suggested that polymers are the long chains that result from the combination of the small repeating units.[1] Throughout the following decades, all polymer researches focused on the development of physical properties of polymers. However, In 1977, Heeger, McDiarmid and Shirakawa found that polymers could also be electrically conductive via doping process.[2] This serendipitous discovery, awarded by Nobel Prize in 2000, was a benchmark which started a new era in polymer science and led to novel applications.

1.1   Conductive/Conjugated Polymers

Until Alan Heeger, Hideki Shirakawa, and Alan MacDiarmid found that polyacetylene (PA) could conduct electricity when doped, all carbon-based polymers were believed to be insulators. In recent decades, such compounds have drawn substantial attention for a wide range of applications such as light-emitting diodes[3], photovoltaics[4], transistors[5], and molecular electronics[6] because of their economic feasibility, suitability, and tunable chemical nature (electronic, optical, conductivity, and stability) provided by the structural design of the precursors. As a result of their potential advantages over the first inorganic electrochromes[7], they have been recognized as one of the most popular electrochromes for usage in devices[8], optical

displays[9], smart windows[10], mirrors[11], and camouflage materials[12], among other applications. Additional properties include a high optical contrast ratio, multicolor printing with the same material, exceptional redox stability, and a long cycle life with minimal response time. A considerable amount of time and effort has been devoted to the design and manufacture of polymeric electrochromics (PECs) based on organic π-conjugated materials as a result of these developments.

The most crucial criteria for being a conducting polymer is the existence of the conjugation through aliphatic backbone. The alternation of single and double bonds between carbon atoms that is responsible for the formation of the backbone of conjugated polymers. When two carbon atoms are linked together in a conjugated polymer chain, one electron per carbon atom is left in the p_z orbital, resulting in three connections with the adjacent atoms. The bilateral overlap of these orbitals provokes electrons to be delocalized all through the conjugation path, leading to the formation of π bonds. As a result of the delocalized electrons filling up the whole band gap, conjugated polymers exhibit intrinsic semiconductor properties.

Because of their numerous advantages over conjugated polymeric materials with an aliphatic backbone, conjugated polymeric materials with an aromatic backbone are far more desired. The stability is the most significant benefit of a conductive polymer with an aromatic backbone. Because of the challenges that scientists and industrialists have had with polyacetylene, along with its poor stability and processability, they have begun to investigate conjugated polymers having an aromatic backbone[13]. Structure of some common conjugated polymers are shown in Figure 1.1.
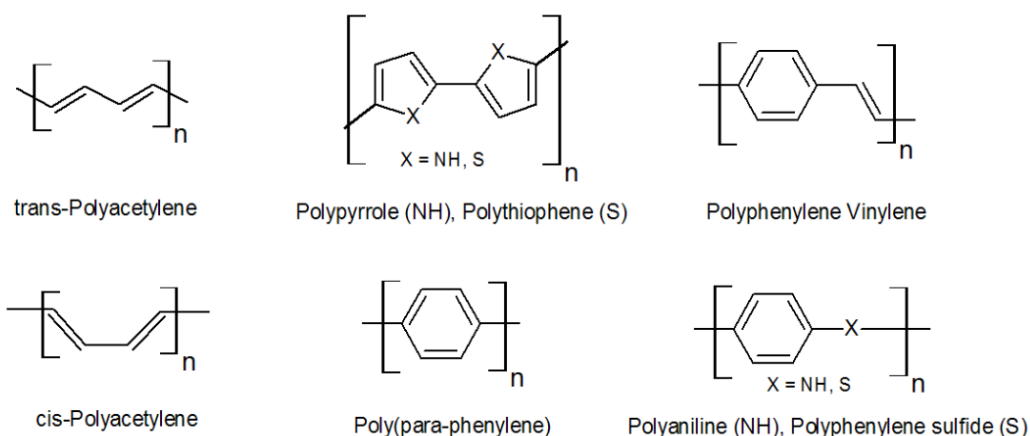
Figure 1.1. Some Common Conjugated Polymers

1.2   Band Gap Theory

There are two discrete energy bands in conjugated polymers: the valence band (VB) and the conduction band (CB). Both optical and electronical properties of conjugated polymers such as color, conductivity, etc. are all affected by the difference in energy between the CB and the VB. The band gap is influenced by a number of factors that can be modified and adjusted. To regulate it, several strategies such as changes in planarity, bond length alternation, resonance effects, and the donor-acceptor approach can be taken into account[14,15]. Tuning the band gap of conducting polymers allows for changes in emission wavelength, absorption in the visible region, and the type of charge carrier produced after doping[16]. It is possible to determine the band gap of conductive polymers by the use of a variety of techniques, such as electroanalytical methods i.e. cyclic voltammetry and differential pulse voltammetry for electronic band gap, as well as spectroelectrochemical techniques for the optical band gap.

1.3   Conductivity and Conduction Mechanism of Conjugated Polymers

Materials can be listed in three categories with respect to their conductivities; metals (conductors), semiconductors and insulators. With a band gap value of less than 3 eV, conducting polymers fall into the semiconductor class, while metals have a zero band gap and insulators have a band gap value greater than 3 eV[11].
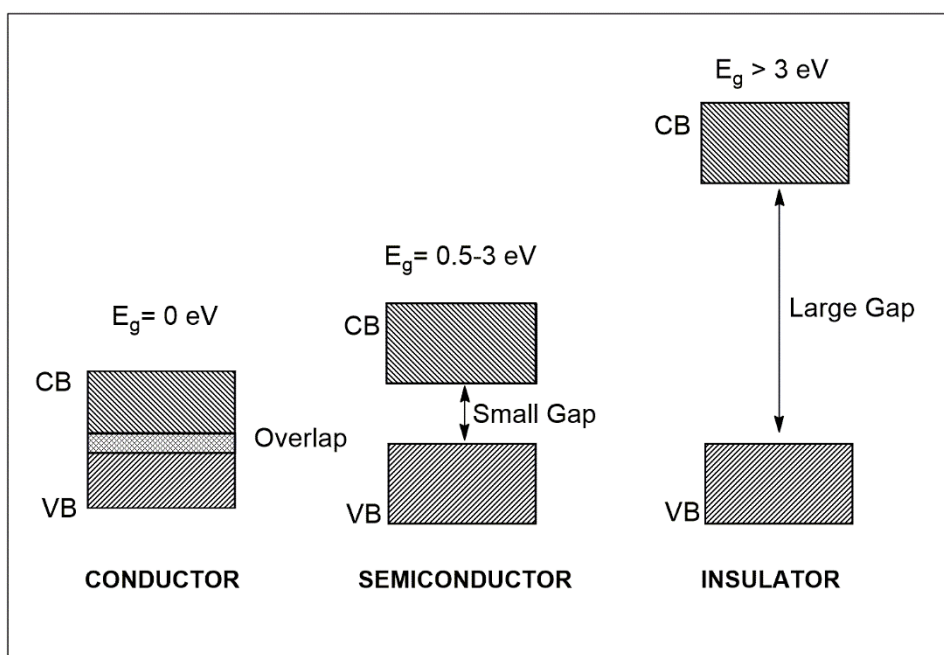
Figure 1.2. Valence Bands and Conduction Bands of Conducting, Semiconducting and Insulating Materials

The intended conductivity of the polymer is typically determined by the area in which it will be used by altering various characteristics of the polymer, primarily the bandgap, of the polymer. Polymers with a low bandgap, for illustration, are particularly well suited for solar cell applications[17].

1.4   Donor-Acceptor Approach

Utilizing a donor acceptor approach is one of the most common methods for lowering the band gap of conductive polymers. A polymer having a delocalized π-electron system that is consisting of repeating electron-rich donor units and electron-deficient acceptor units alternatingly is what is meant by the notion of the donor-acceptor (D-A) approach. The polymer as a whole exhibits a smaller band gap as a consequence of the presence of high-lying HOMO levels of the donor unit in conjunction with low-lying LUMO levels of the acceptor unit(See Figure 1.3). The magnitude of the band gap energy of the polymer may be regulated, and its width can be reduced, depending on the donor and acceptor units that are used[18].
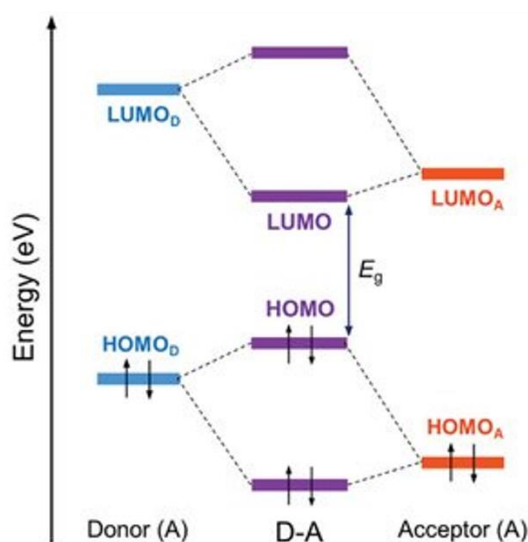
Figure 1.3. Molecular Orbital Interactions of D-A Units

1.5   Solvatochromism

In the field of chemistry, the phenomenon known as solvatochromism refers to the observation that a solute may exhibit more than one color when it is dissolved in a

variety of solvents[19]. When the solvatochromic effect is taken into consideration, the most significant characteristics of the solvent are its dielectric constant and its H bonding capacity. The electronic ground state and excited state of the solute are both affected differently by the different solvents, which is why the magnitude of the energy gap that exists between the two states varies depending on the solvent. This may be seen as variances in the location, intensity, and shape of the spectroscopic bands when looking at both absorption and emission spectra of the solute dissolved in corresponding solvents. Solvatochromism is noticed as a color shift if the spectroscopic band appears in the visible region of the spectrum (See Figure 1.4). If solvents with the increasing polarity leads to a hypsochromic shift, often known as a blue shift, in the absorption or emission spectra, then the negative solvatochromism is corresponded[20].

MeOH, EtOH, *i*-PrOH, MeCN, *t*-BuOH, Me$_2$CO, CHCl$_3$, C$_6$H$_6$

Figure 1.4. Reichardt's Dye Dissolved in Solvents with Different Polarities[21]

1.6   Electrochromism

Electrochromism is the redox driven process by which an external voltage may cause a material to change color in a reversible manner[22]. It is not a requirement that the change in color take place inside the visible spectrum. Moreover, not only the color change but opacity change, transmittance/reflectance change between the redox states also can be taken into the consideration in electrochromism.

In addition to the qualitative observable changes, there are also some parameters defined to quantify the performance of the electrochromic properties. Optical contrast, switching time and coloration efficiency are some of the quantitative properties that measure up the suitibility of the electrochromic devices for the optoelectronic applications.

1.6.1 Optical Contrast

Optical contrast or the electrochromic contrast is the difference in transmittance in terms of percent transmittance change in between the redox states of an electrochromic polymer. It is simply calculated by substracting the percent transmittance value of the bleached state from the value of colored state recorded during chronoabsorptometric experiments(Equation 1-1).

$$\Delta\%T = (\%T_{colored}) - (\%T_{bleached}) \qquad \text{(Equation 1-1)}$$

1.6.2 Switching Time

Switching time is another parameter in electrcrohromism that is defined as the time elapsed during the transitions of an electrochromic polymer between its redox states. In the light of the fact that the human eye is capable of comprehending 95% of the total contrast, switching time is computed by taking this information into account. Switching time is mostly affected with application area, polymer film thickness, ion conducting ability of the electrolyte and ease of diffusion of counter-ions across the polymer chain.

1.6.3 Coloration Efficiency

Coloration Efficiency (η) may be expressed as the total optical density change (ΔOD) for an electrochromic polymer throughout its redox process[23]. This value is calculated in terms of the density of injected or ejected charge (Q_d) during

chronocoulometric and chronoabsorptometric experiments conducted simultaneously using the parameters; transmittance values of colored (T_c) and bleached(T_b) states to obtain optical density change (ΔOD). Following equations are used to calculate the coloration efficiency[24].

$$\Delta OD = \log \frac{T_{bleached}}{T_{colored}} \qquad \text{(Equation 1-2)}$$

$$\eta = \Delta OD / Q_d \qquad \text{(Equation 1-3)}$$

1.7 Literature Survey on Fluorinated Benzothiadizole Acceptor Units

As it is well known, one of the most effective way of controlling the band gap is alternating arrangement of electron donating (D) and electron withdrawing (A) groups along the π-conjugated polymer backbone. In designing push-pull type of polymers, 2,1,3-benzothiadiazole (BTD) molecule is one of the most popular electron deficient units used in organic electronics. To date, numerous conjugated polymers involving the BTD acceptor unit have been synthesized with superior optical and electrochemical properties[25–27]. For example, when the BTD unit is combined with the electron rich 3,4-dioxythiophene based molecules, excellent electrochromic materials are obtained with high optical contrast, fast switching time and high coloration efficiencies[27–29].

Substitution on BTD units plays a crucial role in order to tune some properties of conjugated polymers such as; band gap, molecular weight, inter- and intrachain interactions, charge transport, etc. For example, decreasing the electron density on the benzene ring by introducing electron withdrawing groups on the BTD unit results in both lowering the HOMO and LUMO energy levels, and increasing the inter- and intrachain interactions of the corresponding polymer[27,30,31]. Among various substituents, fluorine atom being most electronegative smallest group is expected to influence both inter and intra molecular interactions[25,32].

The fluorination of BTD unit causes a lowering in Frontier orbitals of a potential D-A polymer[33–35]. With this approach, a notable development in the field has been made in enhancing the performance of organic electronic devices such as improving the power conversion efficiency as well as open circuit voltage, increasing the air stability and color stability of thin film transistors and electroluminescence properties of organic light-emitting diodes[28,36–41]. Therefore, fluorinated BTD derivatives have been the focus of many research papers.

Previously, we have we have investigated the effect of fluorine substitution on BTD acceptor unit in donor-acceptor-donor (D-A-D) type monomers and polymers. For this purpose, monomers containing fluorine substituted benzothiadiazoles as acceptor units and 3,4-ethylenedioxythiophene (EDOT) as donor unit was accomplished via Stille cross-coupling reactions. A blue shift in the electronic absorption spectra of monomers was noted with increasing fluorine atom substitution on the BTD acceptor unit. Morover, an anodic shift was also noted in their oxidation potentials with fluorine atom substitution. This blue shift was also reported by Reynolds *et al*. and explained in terms of deviation from planarity[42]. Y. Yang *et al.* and H. J. Son *et al*. on the other hand, explained the reason of blue shift in terms of steric hindrance between the fluorine atoms on the BTD unit and the neighboring D units for D-A type polymers upon fluorine atom substitution[43,44]. Afterwards, Cihaner *et al*. investigated the effect of fluorine atom substitution on BTD unit in D-A-D type monomers and polymers bearing thiophene donor units. It has been observed that the addition of a fluorine atom led to a lower HOMO energy level in the related polymers, which in turn caused a rise in the electrochemical band gap energy[45]. Despite the fact that the effect of fluorine atom substitution on the BTD unit has previously been systematically investigated, due to reported solubility issues for the obtained polymers, in this study, didecyl substituted ProDOT donor units were coupled with fluorinated and unfluorinated BTD units to overcome the solubility issues.

1.8   Aim of the Study

Although there are several methods to develop a semiconductor which primarily has a low band gap, donor-acceptor approach is the major one to consider. In practice, a donor unit with a high-lying HOMO level and an acceptor with a low-lying LUMO level is preferred. Because the band gap is decreased, the resulting D-A-D type trimeric monomer will have greater conductivity.

From this point of view, the first thought was that increasing the number of electronegative fluorine atoms in the acceptor unit would result in a better electron withdrawing ability when the donor unit remained constant. In parallel, it would allow us to have D-A-D type trimeric monomers with decreasing band gaps as the number of electronegative fluorine atoms in the acceptor unit increased.

Therefore, the goal of this research is to track how the number of fluorine atoms in the acceptor units of D-A-D type trimeric monomers changes their optical, electrochemical, and spectroelectrochemical properties. We synthesized three D-A-D trimeric monomers for this purpose, keeping the donor unit - didecylpropylenedioxythiophene- constant. The sole alteration in the structure of the acceptor unit -benzothiadiazole-, on the other hand, was the gradual increase in the amount of fluorine atoms from zero. We started with the non-fluorinated benzothiadiazole acceptor unit to get D-A-D type monomer 4,7-bis(3,3-didecyl-3,4-dihydro-2H-thieno[3,4-b][1,4]dioxepin-6-yl)benzo[c][1,2,5]thiadiazole **(P0)**, and did proceed with mono- and di- fluorine substituted acceptor units to have two novel derivatives 4,7-bis(3,3-didecyl-3,4-dihydro-2H-thieno[3,4-b][1,4]dioxepin-6-yl)-5-fluorobenzo[c][1,2,5]thiadiazole **(P1)** and 4,7-bis(3,3-didecyl-3,4-dihydro-2H-thieno[3,4-b][1,4]dioxepin-6-yl)-5,6-difluorobenzo[c][1,2,5]thiadiazole **(P2)**. (See Figure 1.2 for the structures of monomers).
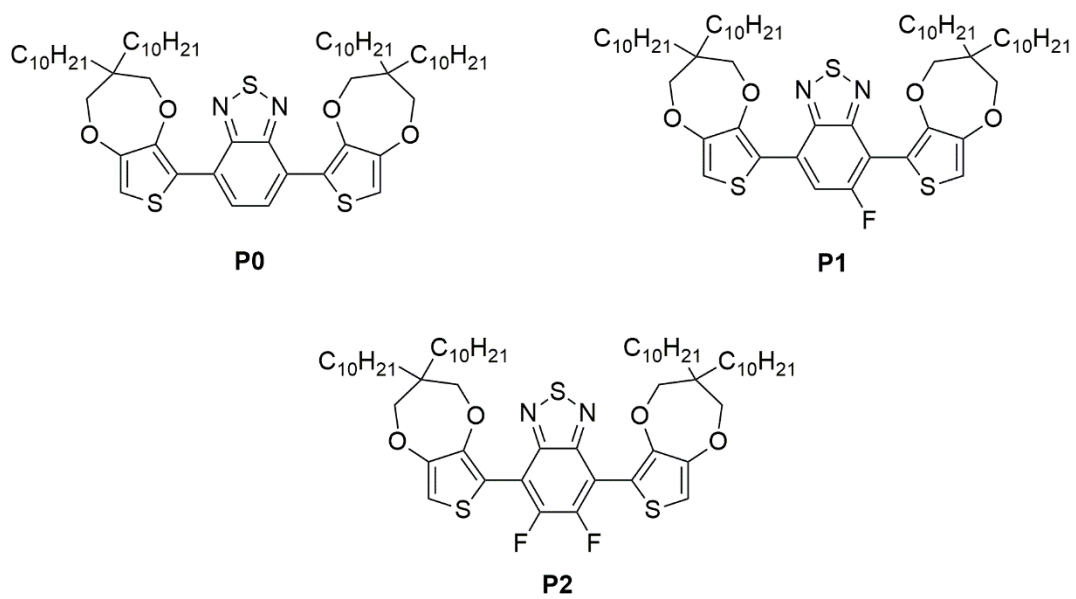
Figure 1.5 Structures of the monomers **P0**, **P1** and **P2**

CHAPTER 2

EXPERIMENTAL

It is preferable to use palladium catalyzed cross-coupling processes for the synthesis of hybrid monomers, which is achieved by coupling two heterocyclic monomers, one of which contains electron donor substituents and the other which has electron withdrawing substituents. The certain kind of cross-coupling reaction varies depending on which reactants are used. In this study, the Stille Cross-Coupling Reaction was employed to execute the coupling reaction between brominated benzothiadiazole based acceptor unit derivatives and didecylpropylenedioxythiophene donor unit after stannylation. To achieve successful synthesis of D-A-D type trimeric monomers via coupling reaction trans-dichloro-bis-triphenylphosphinepalladium ($Pd(PPh_3)_2Cl_2$) was also used as catalyst.

2.1   Synthesis of Monomers

The monomers **P0**, **P1** and **P2** were successfully synthesized by Stille Cross Coupling reaction between stannylated didecyl substituted ProDOT donor unit and 4,7-dibromobenzo[c][1,2,5]thiadiazole, 4,7-dibromobenzo[c][1,2,5]thiadiazole, 4,7-dibromo-5-fluorobenzo[c]   [1,2,5]thiadiazole   and   4,7-dibromo-5,6-difluorobenzo[c][1,2,5]thiadiazole acceptor units.

In order to carry out Stille Cross Coupling reaction, 1 equivalent of the acceptor was dissolved in freshly distilled THF and refluxed half an hour. Then, 2.2 equivalent of donor was added stepwise and refluxed for another half an hour. Lastly, 5% mole of $Pd(PPh_3)_2Cl_2$ catalyst was added to the mixture under nitrogen atmosphere. The final mixture was left in reflux for 48 hours at 70°C. Progress of reaction also monitored

with TLC regularly. Once the reaction has been completed, crude product was taken into the room temperature for cooling. Excess THF in the reaction mixture was evaporated after cooling. After the crude product was transferred into the DCM to extract the organic layer and washed with saturated NaCl solution to get rid of water-soluble impurities. Then the organic layer was dried with anhydrous $MgSO_4$ to remove any leftover water. Residual product was purified with column chromatography according to the procedures stated below for each monomer. Synthetic pathways for the synthesis of each monomer were also given below in Scheme 1, Scheme 2 and Scheme 3 for the monomers **P0**, **P1** and **P2** respectively.

2.1.1 4,7-bis(3,3-didecyl-3,4-dihydro-2H-thieno[3,4-b][1,4]dioxepin-6-yl)benzo[c][1,2,5]thiadiazole (P0)
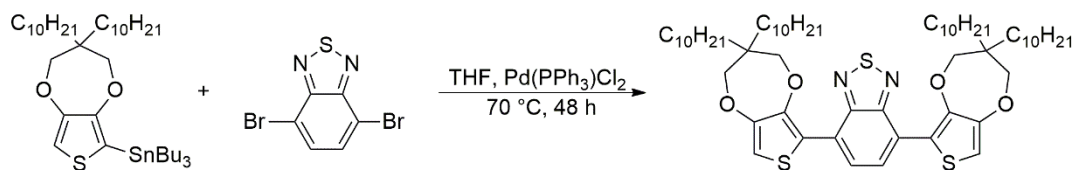
Scheme 1. Synthetic Pathway of **P0**

P0 was obtained as an oily red orange solid with a yield of 60 % by using Hexane:DCM (15:2) as an eluent. ^{1}H NMR (400 MHz, CDCl$_3$, δ (ppm)): 8.28 (s, 2H), 6.64 (s, 2H), 4.04 (s, 4H), 3.95 (s, 4H), 1.49 – 1.40 (m, 8H), 1.35 – 1.21 (m, 64H), 0.88 (t, J = 6.8 Hz, 12H); ^{13}C NMR (100 MHz, CDCl$_3$, δ (ppm)):152.71, 149.89, 147.96, 127.59, 124.32, 117.45, 106.21, 77.80, 77.64, 43.80, 32.00, 31.91, 30.51, 29.65, 29.62, 29.55, 29.34, 22.87, 22.68, 14.11.

2.1.2 4,7-bis(3,3-didecyl-3,4-dihydro-2H-thieno[3,4-b][1,4]dioxepin-6-yl)-5-fluorobenzo[c][1,2,5]thiadiazole (P1)
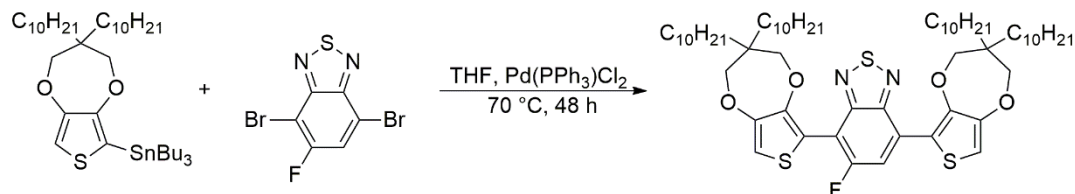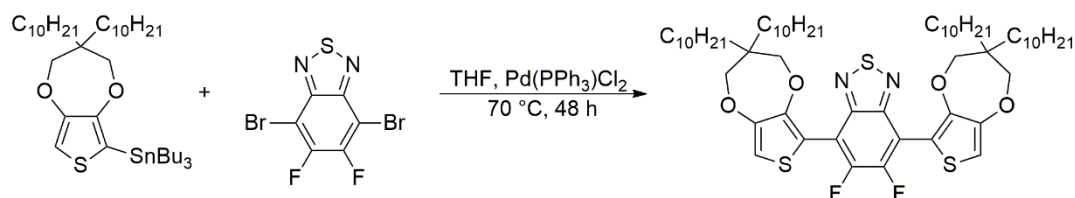

Scheme 2. Synthetic Pathway of **P1**

P1 was obtained as an oily orange compound with a yield of 68 % by using Hexane:DCM (15:2) as an eluent. ^{1}H NMR (400 MHz, CDCl$_3$, δ (ppm)): 8.27 (d, J = 12.1 Hz, 1H), 6.71 (d, J = 10.8 Hz, 2H), 4.07 (s, 2H), 4.00 – 3.89 (m, 6H), 1.49 – 1.35 (m, 8H), 1.35 – 1.19 (m, 64H), 0.92 – 0.83 (m, 12H). ; ^{13}C NMR (100 MHz, CDCl$_3$, δ (ppm)): 161.63, 159.11, 154.58, 149.80, 148.96, 148.42, 126.25, 118.18, 117.85, 115.88, 110.73, 108.46, 107.86, 106.53, 77.85, 77.78, 77.58, 43.93, 43.77, 32.10, 31.93, 31.69, 30.50, 29.66, 29.64, 29.56, 29.36, 22.90, 22.80, 22.71, 14.14. HRMS calculated for C$_{60}$H$_{95}$FN$_2$O$_4$S$_3$, [M]$^+$: 1022.6438. Found for C$_{60}$H$_{95}$FN$_2$O$_4$S$_3$, [M]$^+$: 1022.6559.

2.1.3 4,7-bis(3,3-didecyl-3,4-dihydro-2H-thieno[3,4-b][1,4]dioxepin-6-yl)-5,6-difluorobenzo[c][1,2,5]thiadiazole (P2)

Scheme 3. Synthetic Pathway of **P2**

P2 was obtained as an oily greenish yellow compound with a yield of 62 % by using Hexane:DCM (15:2) as an eluent. ^{1}H NMR (400 MHz, CDCl$_3$, δ (ppm)): 6.68 (s, 2H), 3.86 (d, J = 11.6 Hz 8H), 3.94 – 3.81 (m, 4H), 1.37 – 1.26 (m, 8H), 1.23 – 1.05 (m, 64H), 0.85 – 0.70 (m, 12H) ; ^{13}C NMR (100 MHz, CDCl$_3$, δ (ppm)): 152.18, 150.14, 149.77, 148.99, 111.29, 109.28, 107.57, 77.84, 77.77, 43.94, 31.92, 31.81, 30.50, 29.65, 29.63, 29.55, 29.35, 22.82, 22.70, 14.12. HRMS calculated for C$_{60}$H$_{94}$F$_2$N$_2$O$_4$S$_3$, [M]$^+$: 1040.6344. Found for C$_{60}$H$_{94}$F$_2$N$_2$O$_4$S$_3$, [M]$^+$: 1040.6432.

2.2   Electrochemical Studies of Monomers and Corresponding Polymer Films

Electrochemical studies of monomers were conducted in 0.1 M TBAPF$_6$ dissolved in DCM/ACN mixture by using three-electrode system. Electrochemical studies of monomers **P0**, **P1** and **P2** and electrochemical polymerization of **P0** was accomplished using Pt-disc as working electrode, Ag/AgCl as reference electrode and Pt wire as counter electrode. Electrochemical polymerizaton of **P0** and **P1** and spectroelectrochemical studies of the corresponding polymer films **pP0** and **pP1** were carried out using ITO as working electrode, Ag wire as reference electrode and Pt wire as counter electrode.

CHAPTER 3

RESULTS AND DISCUSSION

The optical and electrochemical properties of the monomers **P0**, **P1**, and **P2** were investigated after their synthesis. Optical properties were investigated using UV-Vis and fluorescence spectrometric methods, while electrochemical properties were investigated using cyclic voltammetry. Then, succesfully obtained polymer films **pP0** and **pP1** were also investigated spectroelectrochemically.

3.1   UV-Vis and Fluorescence Spectra of Monomers

In order to investigate the optical properties of monomers, UV-Vis spectra were recorded in $CHCl_3$ and the resulting spectra are shown in Figure 3.1. (a). As it is seen from the figure, the absorption spectra of the monomers **P0**, **P1** and **P2**, exhibit two different absorption bands. Higher energy bands due to π-π* transition for **P0**, **P1** and **P2** were detected at 317, 309 and 304 nm respectively. Lower energy bands due to the intramolecular charge transfer for **P0**, **P1** and **P2** were detected at 462, 436 and 407 nm respectively[46,47]. Inspection of Figure 1 (a) reveals that the whole spectrum exhibits blue shift with fluorine substitution on the acceptor unit. The shift is more pronounced in the case of lower energy charge transfer band (from 462 nm for **P0** to 407 nm for **P2**).

Emission spectra of the monomers **P0**, **P1** and **P2** were also recorded in $CHCl_3$ and the resulting spectra were given in Figure 3.1(b). Upon excitation at 410 nm, the maximum wavelengths for emission bands were obtained 589, 570 and 548 nm for **P0**, **P1** and **P2** respectively. A similar blue shift trend was also observed as in the case of absorption spectra. These unexpected blue shifts observed in both absorption and emission spectra can be explained with the deviation of planarity due to the steric hindrance caused by fluorine atom substitution to the acceptor unit.
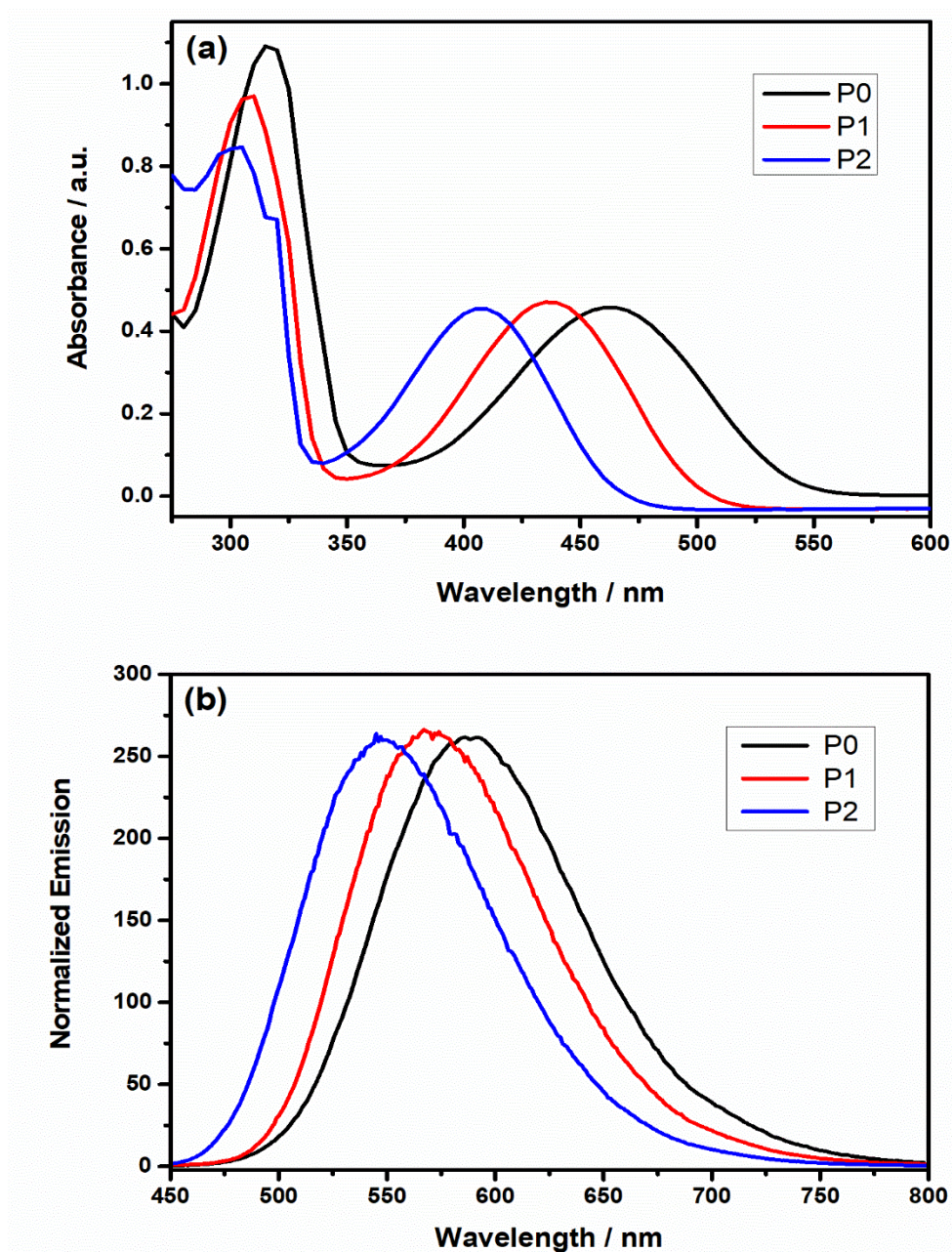
17

Figure 3.1 Absorption (a) and Emission (b) Spectra of the monomers **P0**, **P1** and **P2** in $CHCl_3$ (excited at 410 nm)

In order to prove the existence of ICT band in the absorption spectra of the monomers, fluorescence emission spectra of monomers were recorded in different

solvents having different polarities. The measurements were recorded only for the monomers **P1** and **P2** in hexane, chloroform and DMF. Moving from hexane to DMF, red shifts from 535 nm to 585 nm for **P1** and from 517 nm to 567 nm for **P2** were monitored due to the increasing polarity of the solvents which proves that the lower energy band in their absorption spectra is due to the ICT, indicating strong interactions between donor and acceptor units. Obtained spectra were given in Figure 3.2(a) for **P1** and Figure 3.2(b) for **P2**.

Adding fluorine to the acceptor unit results in a blue shift across the entire spectrum. In the case of lower energy charge transfer bands, the change is more apparent. Although one expects stronger ICT due to increasing acceptor strength upon electronegative fluorine atom substitution to benzothiadiazole unit, this blue shift indicates that ICT between D and A units becomes weaker with fluorine substituted acceptor units. A similar unexpected blue shift was also reported by Reynolds *et al*. and explained in terms of deviation from planarity[42]. Such blue shifts have also been observed and explained on the basis of steric hindrance between the fluorine atoms on the A unit and the adjacent donor units for D-A type polymers following fluorine atom substitution on the acceptor unit[43,44]. Önal *et al*. performed computer simulations in order to gain deeper understanding into the apparent blue shift in the electronic absorption spectra of a series of monomers similar to this study[48]. When fluorine atoms were present, it was found that the planarity of the resulting D-A-D type trimeric monomer was deviated owing to steric hindrance and conformation of the trimeric monomer[41].
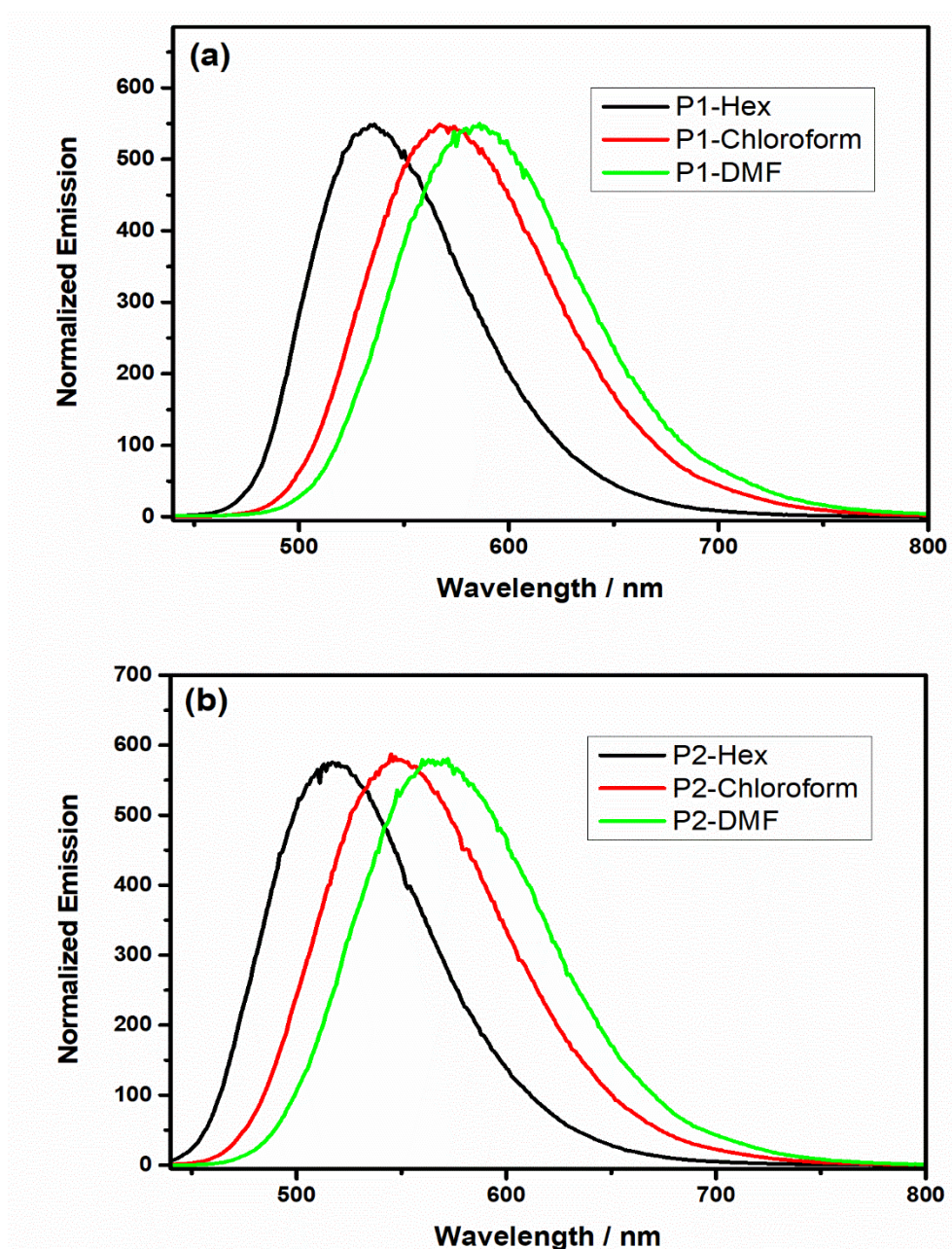
Figure 3.2 Emission Spectra of the monomers (a) **P1** and (b) **P2** in solvents with different polarities

The overall optical properties from the absorption and emission spectra of the monomers **P0**, **P1** and **P2** summarized Table 1.

Table 3.1 Optical Properties of Monomers

Monomers	$\lambda_{max,abs}(nm)$ Hexane	$\lambda_{max,em}(nm)$ Hexane	$\lambda_{max,abs}(nm)$ CHCl$_3$	$\lambda_{max,em}(nm)$ CHCl$_3$	$\lambda_{max,abs}(nm)$ DMF	$\lambda_{max,em}(nm)$ DMF
P0			317, 462	589		
P1	304, 435	535	309, 436	570	436, 308	585
P2	298, 407	517	304, 407	548	405, 300	567

3.2 Electrochemical Properties of Monomers

To investigate the electrochemical properties of monomers, cyclic voltammograms of the monomers **P0**, **P1** and **P2** were recorded in both anodic and cathodic region. The resulting voltammograms are given in Figure 3.3 for (a) **P0** and (b) **P1** and (c) **P2**. As seen in the figures, one irreversible oxidation peak and one reversible reduction peak were noted for each monomers. Irreversible oxidation peaks were found as 1.09 V, 1.34 V and 1.48 V for **P0**, **P1** and **P2** respectively. Reversible reduction peaks were detected as -1.33 V, -1.39 V and -1.42 for **P0**, **P1** and **P2** respectively.

The observed anodic shifts in their oxidation potentials with the increasing number of fluorine atoms in the acceptor unit might be attributed to the lowering of highest occupied molecular orbital (HOMO) energy level upon highly electronegative fluorine atom substitution.

Electrochemical properties of the monomers **P0**, **P1** and **P2** with their oxidation and reduction potentials and onset values were summarized and given in Table 2.
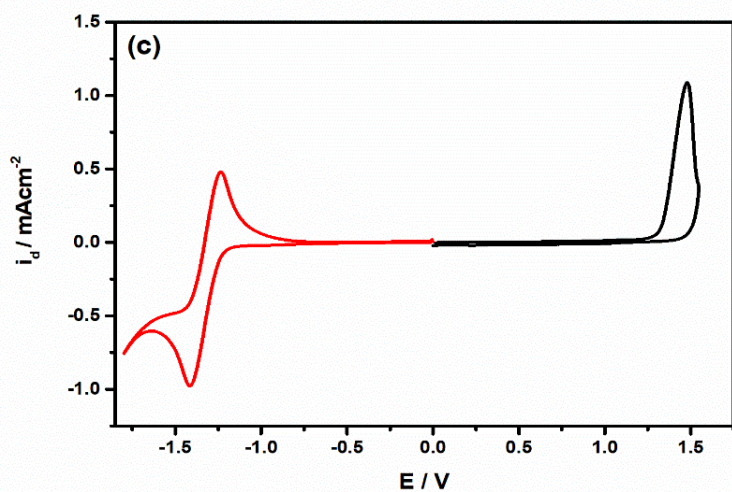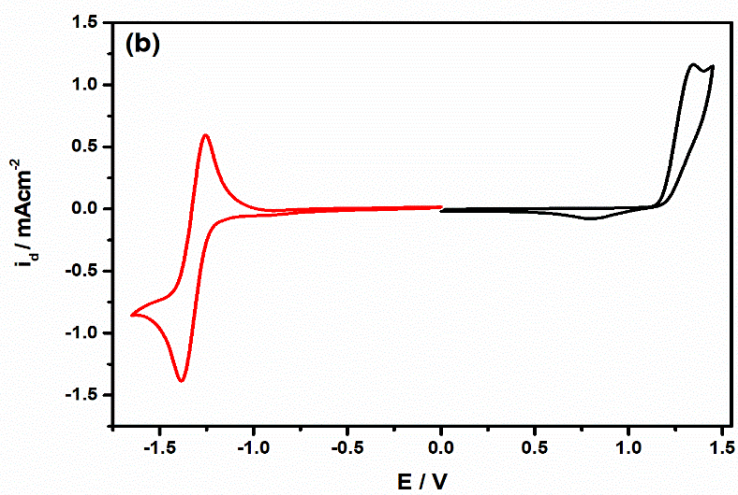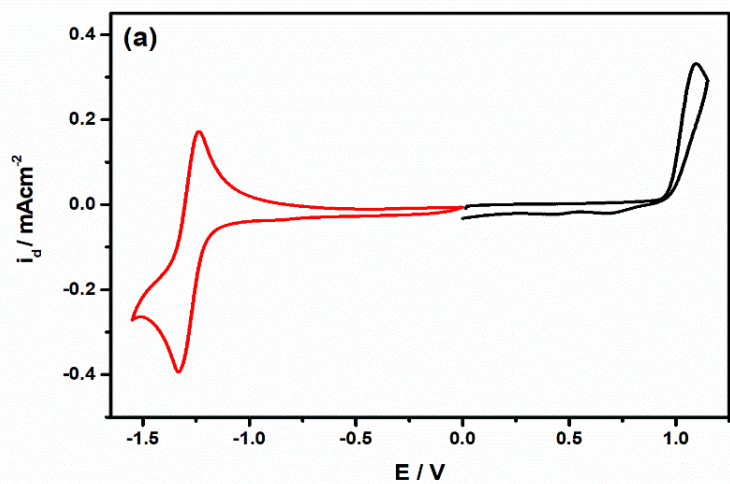
Figure 3.3 Cyclic Voltammograms of the monomers (a) **P0**, (b) **P1** and (c) **P2** recorded in 0.1 M TBAPF$_6$ dissolved in DCM/ACN mixture

Table 3.2 The Electrochemical Properties of the Monomers

Monomers	$E_{ox,m}$ (V)	$E_{ox,onset,m}$ (V)	$E_{red,m}$ (V)	$E_{red,onset,m}$ (V)
P0	1.09	0.96	-1.33	-1.20
P1	1.34	1.17	-1.39	-1.23
P2	1.48	1.33	-1.42	-1.24

3.3 Electrochemical Polymerization of Monomers

P0 and **P1** monomers were polymerized successfully by electrochemical polymerization method using 3-electrode system. On the contrary, although there were many attempts during electrochemical polymerization of **P2** by using many different solvent-electrolyte couples, film formation of the monomer **P2** could not be achieved.

Repetitive cyclic voltammograms recorded during electrochemical polymerization of the monomers were given in Figure 3.4. for (a) **P0** and (b) **P1**. In the figures, it can be observed that new reversible redox couples have been formed. These new peaks became more prominent as the anodic scans progressed, and they indicate the generation of electroactive polymer films on the working electrode surface, with the thickness of the film rising with time.

When the polymer films were formed on ITO coated glass working electrodes, the electrochemical behavior of the polymer films was evaluated by recording their cyclic voltammograms in a fresh electrolyte solution in order to investigate the function of fluorine atom substitution. In order to do this, polymer films were deposited on the electrode surface using a potential cycling between 0.0 V to +1.15 vs Ag/AgCl for **P0**, 0.0 V to +1.4 V vs Ag/AgCl for **P1**.
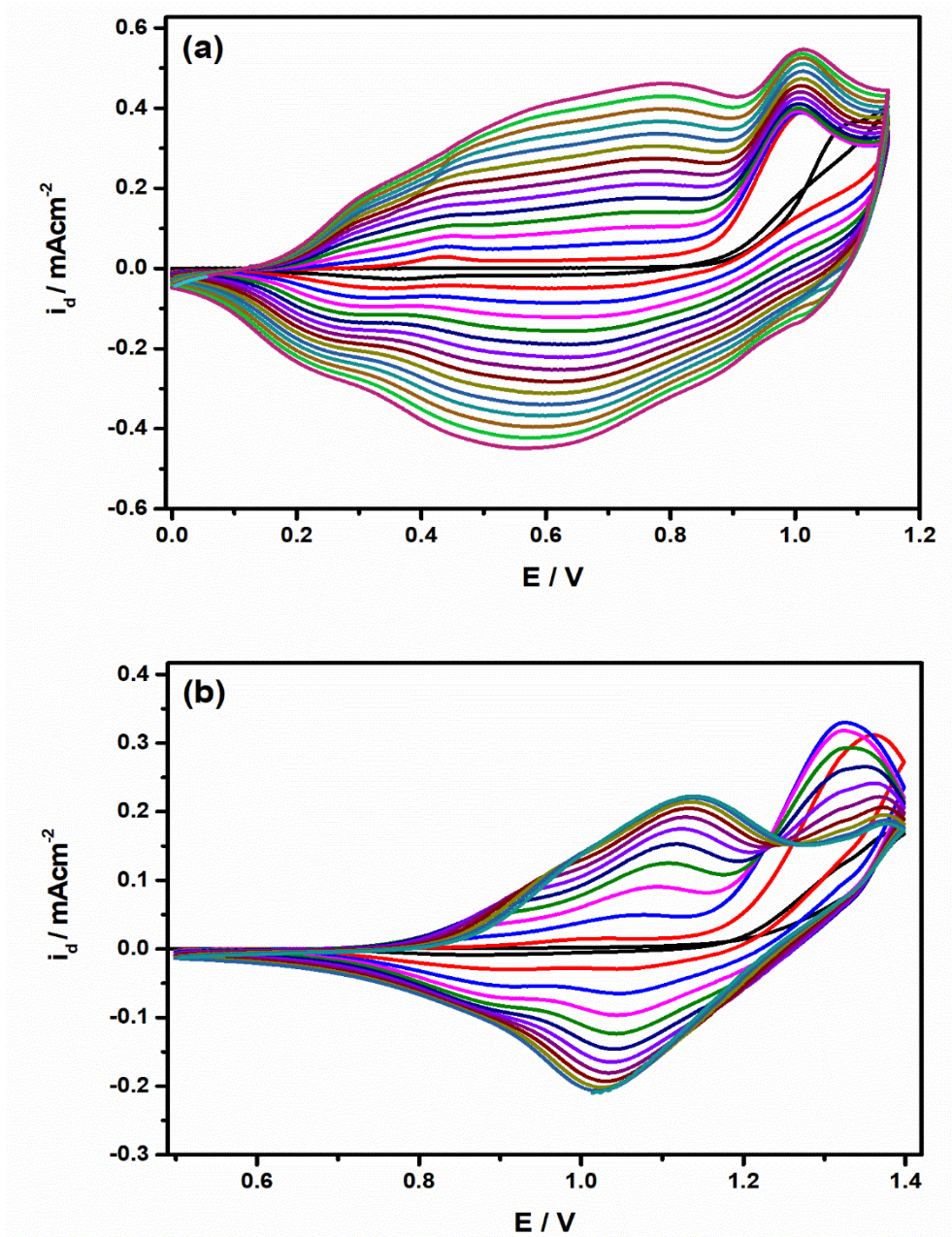
Figure 3.4 cyclic voltammograms of (a) **P0** and (c) **P1** monomer recorded in 0.1 M TBAPF6 in DCM/MeCN (1/1: v/v) on ITO electrode at a scan rate of 100 mV/s.

24

3.4 Electrochemical Properties of Polymer Films

Following the conclusion of polymer film production, the polymer films deposited working electrodes were washed with ACN to eliminate any leftover monomer or oligomeric species, and the cyclic voltammograms of the freshly formed polymer films were recorded. It can be observed from the voltammograms displayed in Figure 5 that polymer films **pP0** and **pP1** revealed one reversible oxidation peak at 1.02 V and 1.22 V respectively.
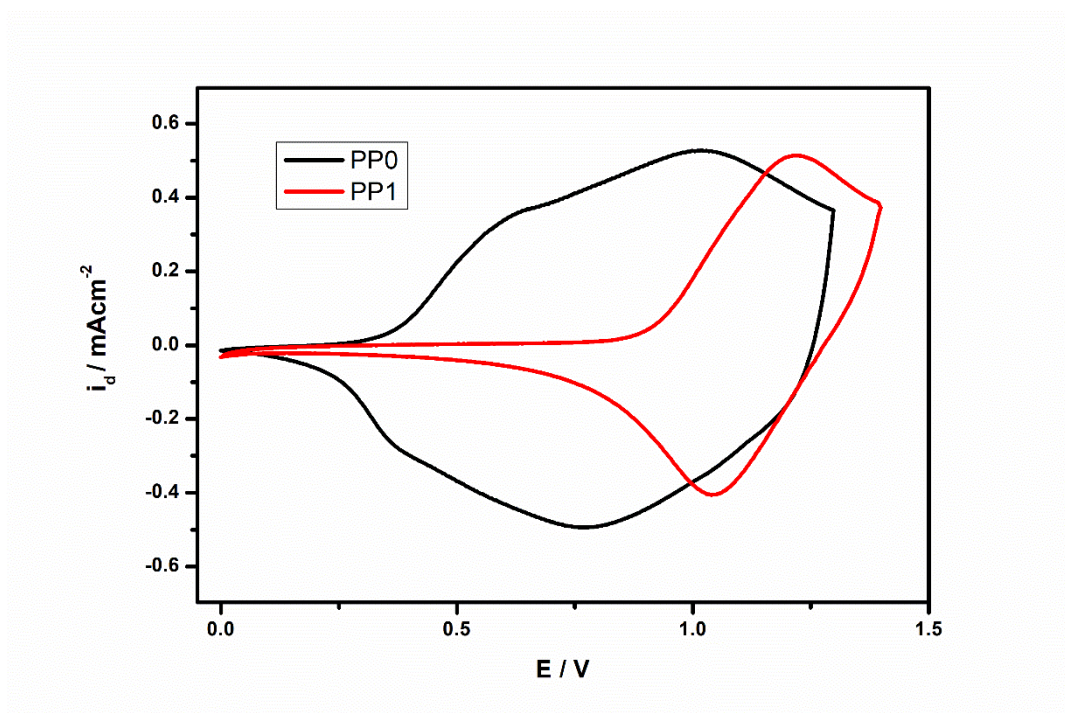

Figure 3.5 voltammograms of the corresponding polymer films **pP0** and **pP1** recorded in 0.1 M TBAPF$_6$ in ACN on ITO electrode at a scan rate of 100 mV/s.

3.5 Scan Rate Dependence of Polymer Films

A further investigation into the scan rate dependency of anodic and cathodic peak currents was carried out by measuring the current variations of polymer film coated

electrodes at different scan rates ranging from 20 to 200 mV/s. As a function of voltage scan rates, a linear increase was noted in the peak currents of the redox couples, which not only demonstrated the presence of well-adhered polymer films on the ITO coated glass electrodes, but also demonstrated that the redox processes generated by doping and de-doping of polymer films are not diffusion controlled.
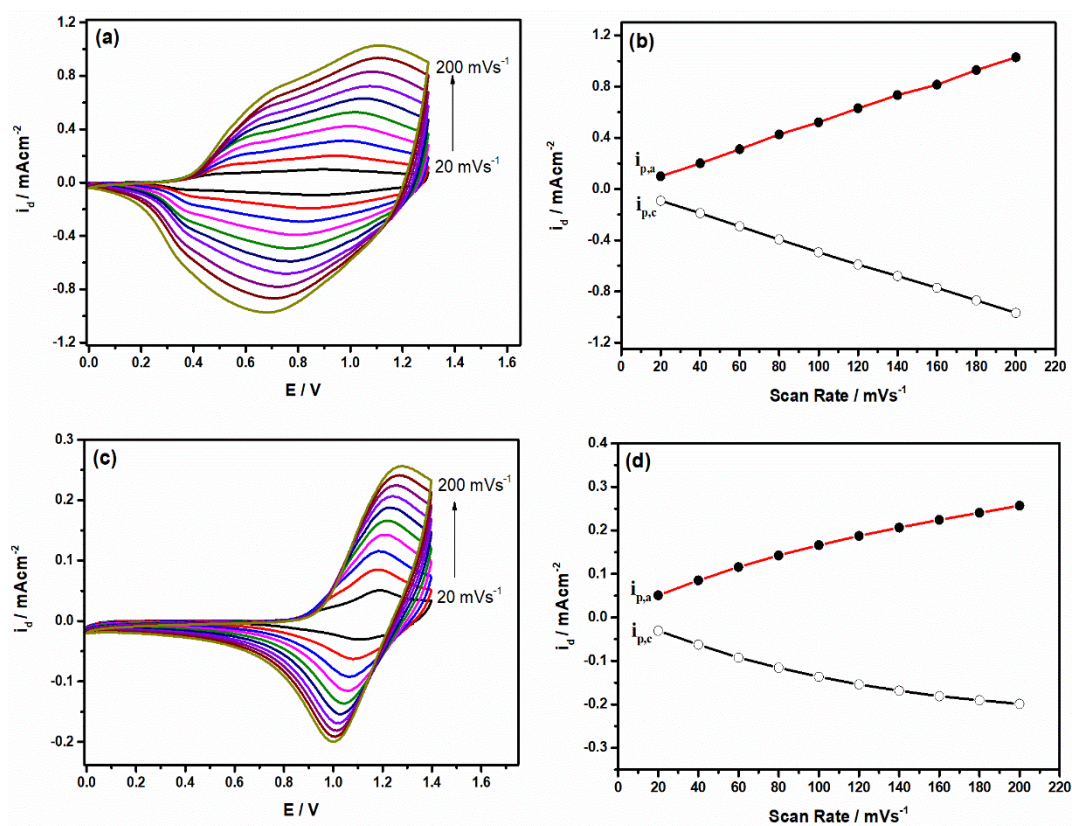

Figure 3.6 Scan rate dependence of the polymer films on ITO electrode recorded in 0.1 M TBAPF$_6$ solution in ACN (a) **pP0** and (c) **pP1** in at different scan rates with 20 mV/s increments from 20 mV/s to 200 mV/s. The relationship of anodic and cathodic current peaks as a function of scan rate for (b) **pP0** and (d) **pP1** polymer films.

26

3.6   Spectroelectrochemical Properties of Polymer Films

For the purpose of investigation of optoelectronic characteristics of the polymer films **pP0** and **pP1**, spectroelectrochemical measurements were carried out via simultaneous use of both cyclic voltammetry and UV-Vis spectrometry. The neutral state absorption spectra of **pP0** and **pP1** films deposited on ITO-glass electrode were compared in Figure 3.7. Following a close examination of the figure, it was observed that both of the polymer films display dual-band absorption, which is characteristic of D-A polymers.
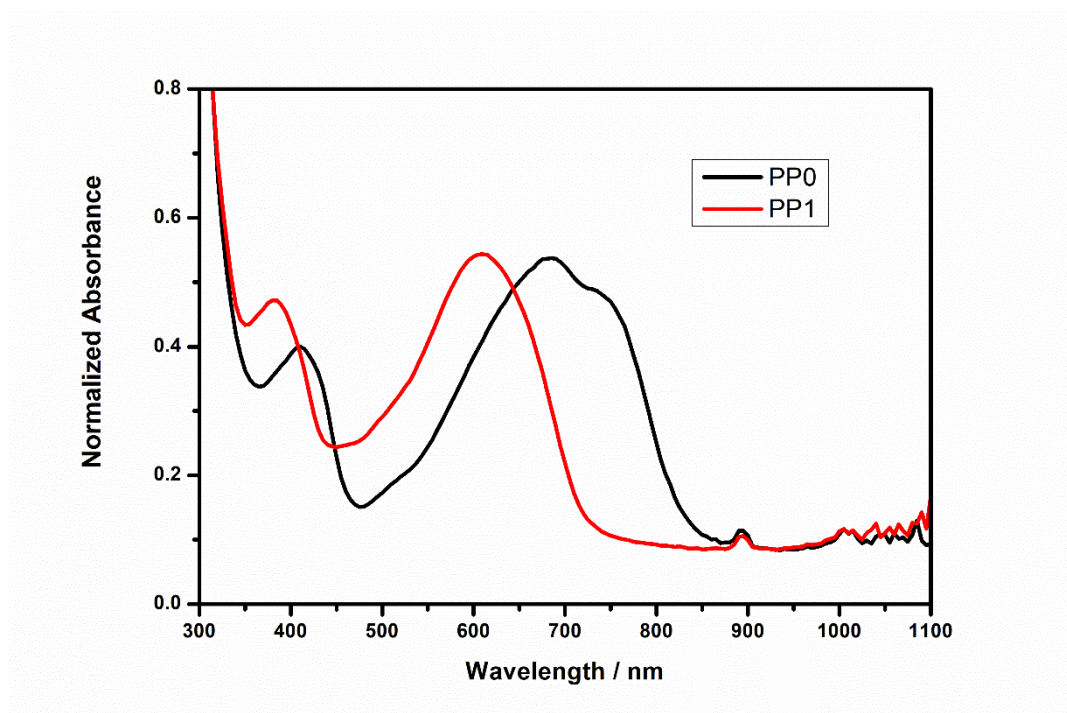

Figure 3.7 Neutral state absorption spectra of polymer films **pP0** and **pP1** coated on ITO electrode in 0.1 M TBAPF$_6$/ACN.

Two discrete absorption bands were observed at their neutral states in higher energy and lower energy region due to π- π^* and ICT interactions respectively. Higher energy bands were found to appear at 410 nm and 380 nm, while lower energy bands

were determined as 680 nm and 610 nm for the polymer films **pP1** and **pP2** respectively.

We have noticed blue shifts in the electronic absorption spectra of polymer films, similar to those found in the electronic absorption spectra of monomers, when the number of F atoms on the acceptor units of polymer films increases. Fluorine substituted polymers have also been shown to exhibit comparable blue shifts in the literature[32,49,50,].

The optical band gap values (E_g) of the polymers were derived from the onset of the low energy band and determined to be 1.48 V and 1.70 V for the polymers **pP0** and **pP1** respectively (see Table 2). A number of cases have also been reported in which the optical band gap values have increased with increasing backbone fluorination, and this has been linked to a shorter effective conjugation length[32].

In order to investigate the optoelectronic behavior of polymer films, it was necessary to follow the changes in their electronic absorption spectra as a function of applied voltage, and the resultant spectra recorded for **pP0** and **pP1**, are shown in Figure 3.8(a) and (b) respectively. Detailed examination of Figure 3.8 revealed that the intensity of the π-π* transition bands **pP0** and **pP1** polymer films decreased concurrently, with corresponding absorption bands forming at around 900 nm for both **pP1** and **pP2**, respectively, during p-doping of the **pP0** and **pP1** films, suggesting the generation of charge carriers. The presence of clear isosbestic spots at 805 nm and 700 nm during the early phases of oxidation of **pP0** and **pP1** films, respectively, shows that polymer films were being interconverted between their neutral and oxidized states during this time period. On the other hand, with further oxidation of **pP0** and **pP1**, these points change with the introduction of additional absorption bands beyond 1000 nm for both **pP0** and **pP1**, which is most likely a result of bipolaron production[29,51].

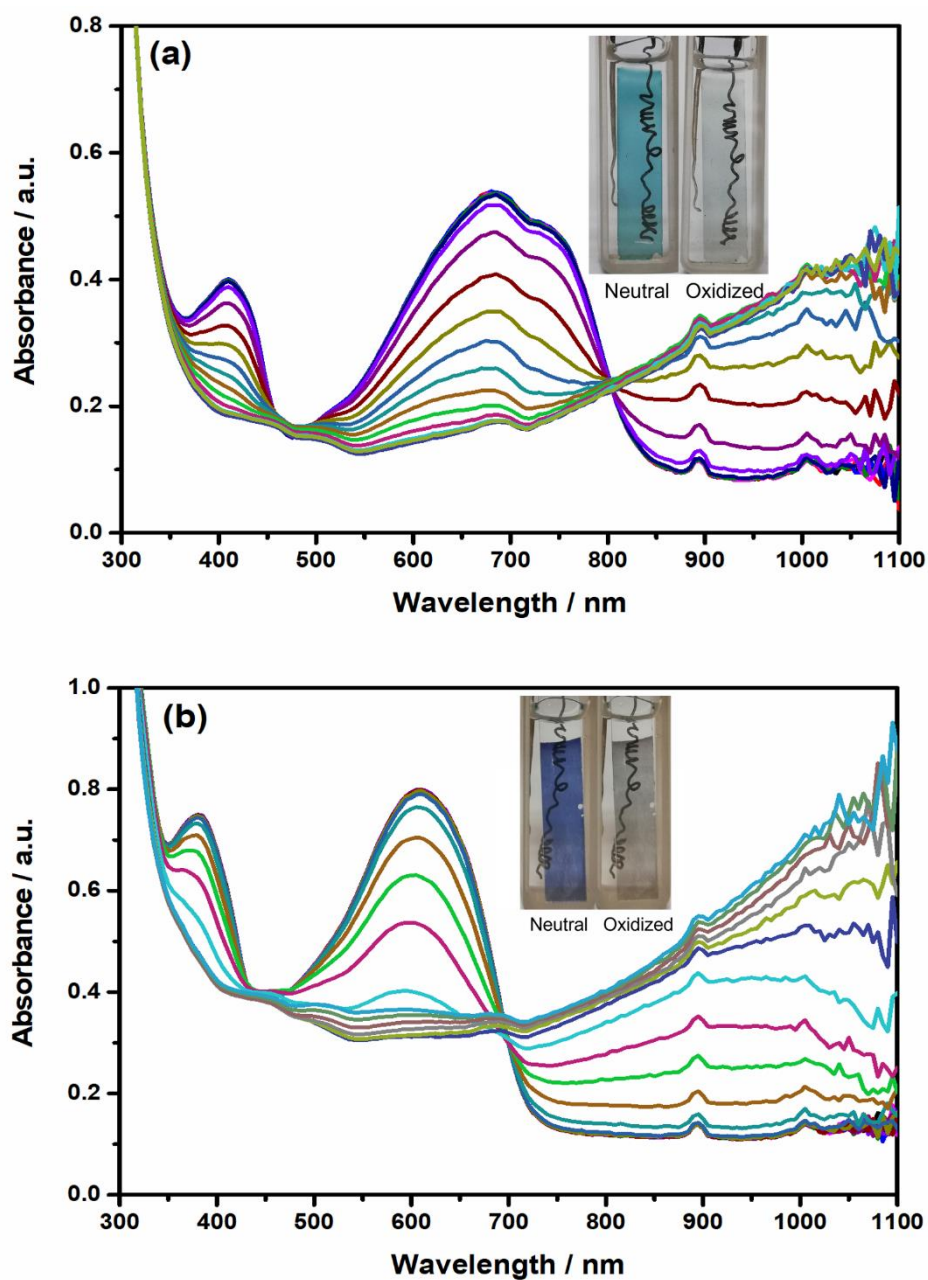Figure 3.8 The changes in electronic absorption spectra of electrochemically deposited (a) **pP0** and (b) **pP1** films on ITO recorded at various applied potentials in 0.1 M TBAPF$_6$/ACN. Inset: The colors of the films at neutral and oxidized states.

Polymer films **pP0** and **pP1** show aqua green and navy blue in their neutral states and transparent gray and less transparent gray respectively when oxidized.

3.7   Kinetic Studies of Polymer Films

The percent transmittance change also known as the optical contrast of polymer films **pP0** and **pP1** was investigated using the square wave potential technique. For this aim, the polymer films were first neutralized, then oxidized repetitively, with each step taking 10 seconds. Corresponding spectra of the polymer films **pP0** and **pP1** are given in Figure 3.9. **pP0** and **pP1** polymer films exhibited optical contrast values of 38% and 26% for lower energy absorption bands and 25% and 14% for higher energy absorption bands.
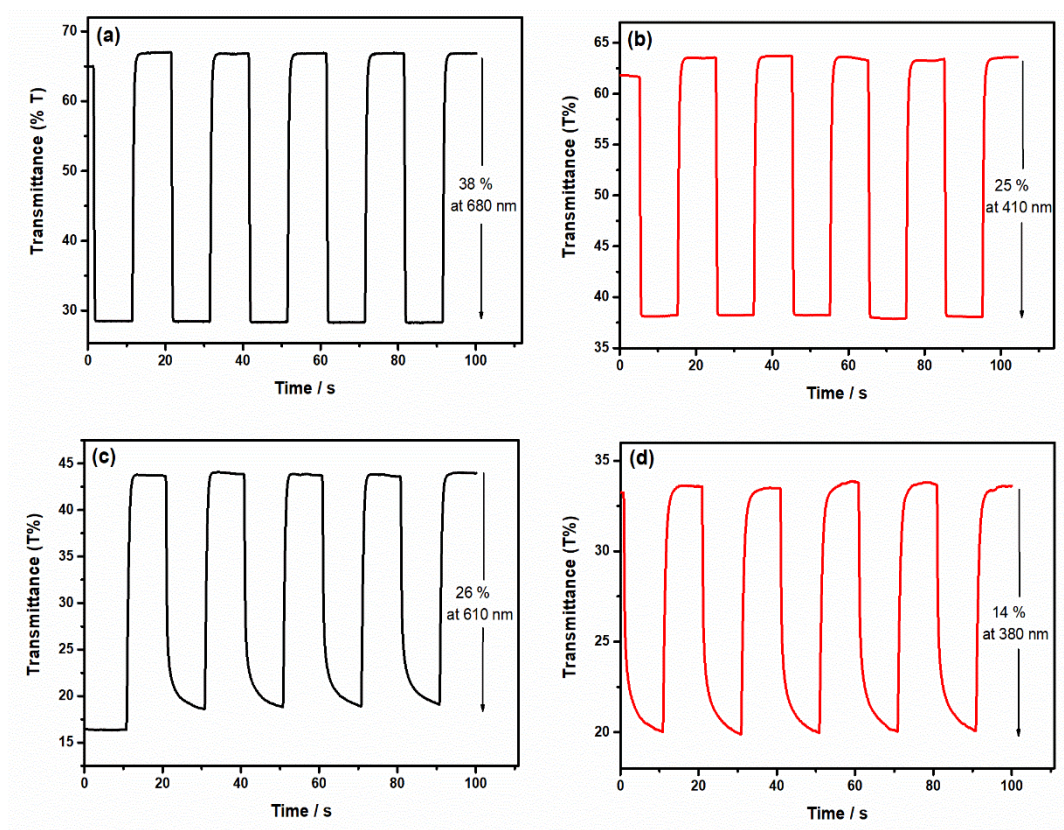

Figure 3.9 Chronoabsorptometry experiments for the polymer films **pP0** and **pP1** on ITO in 0.1 M TBAPF$_6$/ACN when the films were switched between redox states with an interval time of 10 s for **pP0** at (a) 680 nm and (b) 410 nm, for **pP1** at (c) 610 nm and (d) 380 nm.

Table 3.3 The Electrochemical and Optical Properties of the Polymers

Polymers	$E_{ox,p}$ (V)	$E_{ox,p,onset}$ (V)	λ_{max} (nm)	$\Delta\%T$	CE (cm2/C)	E_g^a (eV)	t_s^b (s)	Color at neutral state	Color at oxidized state
P0	1.02	0.37	410, 680	25, 38	207, 385	1.48	0.6, 0.7	Aqua Green	Transparent Gray
P1	1.22	0.91	380, 610	14, 26	114, 205	1.70	1.0, 1.4	Navy Blue	Transparent Gray

[a] Optical band gap.
[b] 95% of full switch from colored to bleached states.

Moreover, the switching time (ts), which is the time required to achieve 95 % of the maximum change in optical contrast upon application of a potential, was determined to be 0.6 and 1.0 s for the higher energy absorption band and 0.7 and 1.4 s for the lower energy absorption band for the **pP0** and **pP1** films, respectively.

The coloration efficiencies (CEs) of the polymer films were also calculated and found to be 207 cm^2/C at 410 nm and 385 cm^2/C at 680 nm for **pP0** and 114 cm^2/C at 380 nm and 205 cm^2/C at 610 nm for **pP1**.

CHAPTER 4

CONCLUSION

In this thesis study, three trimeric monomers in D-A-D configuration was synthesized using non-, mono- and di-fluorinated benzothiadiazole acceptor units to investigate the effect of number of fluorine atoms attached on the acceptor unit. Didecylpropylenedioxythiophene donor unit was chosen to obtain soluble polymers. In an effort to inspect the electronegative fluorine atom substitution on the benzothiadiazole unit, optical and electrochemical properties of the monomers were investigated. Deviation from planarity possibly caused by the steric hindrance due to the increasing number of fluorine atoms on the acceptor unit led to a blue shift in both absorption and emission spectra of the monomers **P1** and **P2** when compared to non-fluorinated analogue, **P0.** Fluorine atom substitution was observed to lower the HOMO levels of monomers, thereby, resulting in an increase in monomer oxidation potential. Aside from significant variances in the optical and electrochemical properties of the monomers, respective corresponding polymer films also exhibited noteworthy variations in their optoelectronic properties. A blue shift was observed with increased addition of F atoms onto the polymer backbone, similar to what had been noticed in the electronic absorption spectra of monomers(i.e. 462 nm for **P0**, 436 nm for **P1** in $CHCl_3$). This is also accompanied by a broadening of the band gap(i.e. 1.48 eV and 1.70 eV for **pP0** and **pP1** respectively). Even though the electrochromic polymer films were found to have comparable and reasonably short switching times, the CEs of the films decreased when the number of F atoms added to the polymer backbone was increased.

REFERENCES

1. Percec, V. & Xiao, Q. The Legacy of Hermann Staudinger: Covalently Linked Macromolecules. *Chem* **6**, 2855–2861 (2020).

2. Hideki Shirakawa, B., Louis, E. J., Macdiarmid, A. G., Chiang, C. H. & Heeger, A. J. Synthesis of Electrically Conducting Organic Polymers : Halogen Derivatives of Polyacetylene, $(CH)_x$. *Chem. Comm.* **474**, 578-580 (1977).

3. Friend, R., Gymer, R., Holmes, A. *et al.* Electroluminescence in conjugated polymers. *Nature* **397,** 121–128 (1999). https://doi.org/10.1038/16393

4. Schmidt-Mende, L. *et al.* Self-organized discotic liquid crystals for high-efficiency organic photovoltaics. *Science (1979)* **293**, 1119–1122 (2001).

5. Gao, P. *et al.* Benzo[1,2-b:4,5-b′]bis[b]benzothiophene as solution processible organic semiconductor for field-effect transistors. *Chemical Communications* 1548–1550 (2008) doi:10.1039/b717608b.

6. Palma, M. *et al.* Self-organization and nanoscale electronic properties of azatriphenylene-based architectures: A scanning probe microscopy study. *Advanced Materials* **18**, 3313–3317 (2006).

7. Beaupré, S., Breton, A. C., Dumas, J. & Leclerc, M. Multicolored electrochromic cells based on poly(2,7-carbazole) derivatives for adaptive camouflage. *Chemistry of Materials* **21**, 1504–1513 (2009).

8. Schwendeman, I. *et al.* Enhanced contrast dual polymer electrochromic devices. *Chemistry of Materials* **14**, 3118–3122 (2002).

9. Bange, K. & Gambke, T. Electrochromic Materials for Optical Switching Devices. *Advanced Materials 2* **1**, 10-16 (1990)

10. Pennisi, A., Simone, F., Barletta, G., Marco, G. di & Lanza, M. Preliminary test of a large electrochromic window. *Electrochimica Acta* **44**, 3237-3243 (1999)

11. Rosseinsky, D. R. & Mortimer, R. J. Electrochromic Systems and the Prospects for Devices. Advanced Materials **13(11)**, 783-793 (2001)

12. Chandrasekhar, P. *et al.* Large, Switchable Electrochromism in the Visible Through Far-Infrared in Conducting Polymer Devices. Adv. Funct. Mater. **12**, 95-103 (2002)

13. Eken, S., Ergun, E. G. C. & Önal, A. M. Synthesis and Electrochemical Polymerization of Dithienosilole-Based Monomers Bearing Different Donor Units. *Journal of The Electrochemical Society* **163**, G69–G74 (2016).

14. Havinga, E., ten Hoeve, W. & Wynberg, H. A new class of small band gap organic polymer conductors. *Polymer Bulletin* **29,** (1992).

15. Roncali, J. Synthetic Principles for Bandgap Control in Linear π-Conjugated Systems. *Chem. Rev.* **97**, 173-205 (1997)

16. Özkut, M. İ. Color Engineering of Π-Conjugated Donor-Acceptor Systems: The Role of Donor and Acceptor Units on the Neutral State Color (2011).

17. Bakhshi, A. K., Kaur, A. & Arora, V. Molecular engineering of novel low band gap conducting polymers. *Indian Journal of Chemistry* **51**, 57-68 (2012)

18. Gibson, G. L., McCormick, T. M. & Seferos, D. S. Atomistic band gap engineering in donor-acceptor polymers. *J. Am. Chem. Soc.* **134**, 539–547 (2012).

19. Marini, A., Muñoz-Losa, A., Biancardi, A. & Mennucci, B. What is solvatochromism? *Journal of Physical Chemistry B* **114**, 17128–17135 (2010).

20.   Kulinich, A. v., Mikitenko, E. K. & Ishchenko, A. A. Scope of negative solvatochromism and solvatofluorochromism of merocyanines. *Physical Chemistry Chemical Physics* **18**, 3444–3453 (2016).

21.   Afri, M., Gottlieb, H. E. & Frimer, A. A. Reichardt's dye: The NMR story of the solvatochromic betaine dye. *Canadian Journal of Chemistry* **92**, 128–134 (2014).

22.   Kraft, A. Electrochromism: a fascinating branch of electrochemistry. *ChemTexts* **5**, (2019).

23.   Rojas-González, E. A. & Niklasson, G. A. Differential coloration efficiency of electrochromic amorphous tungsten oxide as a function of intercalation level: Comparison between theory and experiment. *Journal of Applied Physics* **127**, 205101 (2020).

24.   Argun, A. A. *et al.* Multicolored electrochromisin in polymers: Structures and devices. *Chemistry of Materials* vol. 16 4401–4412 (2004).

25.   Nielsen, C. B., White, A. J. P. & McCulloch, I. Effect of Fluorination of 2,1,3-Benzothiadiazole. *Journal of Organic Chemistry* **80**, 5045–5048 (2015).

26.   Gong, X., Li, G., Li, C., Zhang, J. & Bo, Z. Benzothiadiazole based conjugated polymers for high performance polymer solar cells. *Journal of Materials Chemistry A* **3**, 20195–20200 (2015).

27.   Ledwon, P. *et al.* The role of structural and electronic factors in shaping the ambipolar properties of donor-acceptor polymers of thiophene and benzothiadiazole. *RSC Advances* **5**, 77303–77315 (2015).

28.   Vasilyeva, S. v. *et al.* Material strategies for black-to-transmissive window-type polymer electrochromic devices. *ACS Applied Materials and Interfaces* **3**, 1022–1032 (2011).

29.	Durmus, A., Gunbas, G. E., Camurlu, P. & Toppare, L. A neutral state green polymer with a superior transmissive light blue oxidized state. *Chemical Communications* 3246–3248 (2007) doi:10.1039/b704936f.

30.	Zhou, P., Zhang, Z. G., Li, Y., Chen, X. & Qin, J. Thiophene-fused benzothiadiazole: A strong electron-acceptor unit to build D-A copolymer for highly efficient polymer solar cells. *Chemistry of Materials* **26**, 3495–3501 (2014).

31.	Nielsen, C. B. *et al.* 2,1,3-benzothiadiazole-5,6-dicarboxylic imide - A versatile building block for additive- and annealing-free processing of organic solar cells with effi ciencies exceeding 8%. *Advanced Materials* **27**, 948–953 (2015).

32.	Neo, W. T., Ong, K. H., Lin, T. T., Chua, S. J. & Xu, J. Effects of fluorination on the electrochromic performance of benzothiadiazole-based donor - Acceptor copolymers. *Journal of Materials Chemistry C* **3**, 5589–5597 (2015).

33.	Hu, H. *et al.* Terthiophene-Based D-A Polymer with an Asymmetric Arrangement of Alkyl Chains That Enables Efficient Polymer Solar Cells. *J Am Chem Soc* **137**, 14149–14157 (2015).

34.	Jo, J. W., Bae, S., Liu, F., Russell, T. P. & Jo, W. H. Comparison of two D-A type polymers with each being fluorinated on D and A unit for high performance solar cells. *Advanced Functional Materials* **25**, 120–125 (2015).

35.	Iyer, A., Bjorgaard, J., Anderson, T. & Köse, M. E. Quinoxaline-based semiconducting polymers: Effect of fluorination on the photophysical, thermal, and charge transport properties. *Macromolecules* **45**, 6380–6389 (2012).

36. Wang, B. *et al.* Heteroatom substituted naphthodithiophene-benzothiadiazole copolymers and their effects on photovoltaic and charge mobility properties. *Polymer Chemistry* **6**, 4479–4486 (2015).

37. Wang, X. *et al.* Effects of fluorination on the properties of thieno[3,2-b]thiophene-bridged donor-π-acceptor polymer semiconductors. *Polymer Chemistry* **5**, 502–511 (2014).

38. Lei, T. *et al.* Ambipolar polymer field-effect transistors based on fluorinated isoindigo: High performance and improved ambient stability. *J Am Chem Soc* **134**, 20025–20028 (2012).

39. Giovanella, U. *et al.* Perfluorinated polymer with unexpectedly efficient deep blue electroluminescence for full-colour OLED displays and light therapy applications. *Journal of Materials Chemistry C* **1**, 5322–5329 (2013).

40. Shen, P., Bin, H., Zhang, Y. & Li, Y. Synthesis and optoelectronic properties of new D-A copolymers based on fluorinated benzothiadiazole and benzoselenadiazole. *Polymer Chemistry* **5**, 567–577 (2014).

41. Schroeder, B. C. *et al.* Silaindacenodithiophene-based low band gap polymers - The effect of fluorine substitution on device performances and film morphologies. *Advanced Functional Materials* **22**, 1663–1670 (2012).

42. Steckler, T. T., Abboud, K. A., Craps, M., Rinzler, A. G. & Reynolds, J. R. Low band gap EDOT-benzobis(thiadiazole) hybrid polymer characterized on near-IR transmissive single walled carbon nanotube electrodes. *Chemical Communications* 4904–4906 (2007) doi:10.1039/b709672k.

43. You, J. *et al.* A polymer tandem solar cell with 10.6% power conversion efficiency. *Nature Communications* **4**, (2013).

44. Yun, J. H. *et al.* Enhancement of charge transport properties of small molecule semiconductors by controlling fluorine substitution and effects on

photovoltaic properties of organic solar cells and perovskite solar cells. *Chemical Science* **7**, 6649–6661 (2016).

45. Çakal, D., Ercan, Y. E., Önal, A. M. & Cihaner, A. Effect of fluorine substituted benzothiadiazole on electro-optical properties of donor-acceptor-donor type monomers and their polymers. *Dyes and Pigments* **182**, (2020).

46. Içli-Özkut, M., Ipek, H., Karabay, B., Cihaner, A. & Önal, A. M. Furan and benzochalcogenodiazole based multichromic polymers via a donor-acceptor approach. *Polymer Chemistry* **4**, 2457–2463 (2013).

47. Wang, E. *et al.* Donor polymers containing benzothiadiazole and four thiophene rings in their repeating units with improved photovoltaic performance. *Macromolecules* **42**, 4410–4415 (2009).

48. Çakal, D., Boztaş, Y., Akdag, A. & Önal, A. M. Investigation of Fluorine Atom Effect on Benzothiadiazole Acceptor Unit in Donor Acceptor Donor Systems. *Journal of The Electrochemical Society* **166**, G141–G147 (2019).

49. Umeyama, T., Watanabe, Y., Douvogianni, E. & Imahori, H. Effect of fluorine substitution on photovoltaic properties of benzothiadiazole-carbazole alternating copolymers. *Journal of Physical Chemistry C* **117**, 21148–21157 (2013).

50. Zhou, H. *et al.* Development of fluorinated benzothiadiazole as a structural unit for a polymer solar cell of 7% efficiency. *Angewandte Chemie - International Edition* **50**, 2995–2998 (2011).

51. Baran, D., Oktem, G., Celebi, S. & Toppare, L. Neutral-state green conjugated polymers from pyrrole bis-substituted benzothiadiazole and benzoselenadiazole for electrochromic devices. *Macromolecular Chemistry and Physics* **212**, 799–805 (2011).
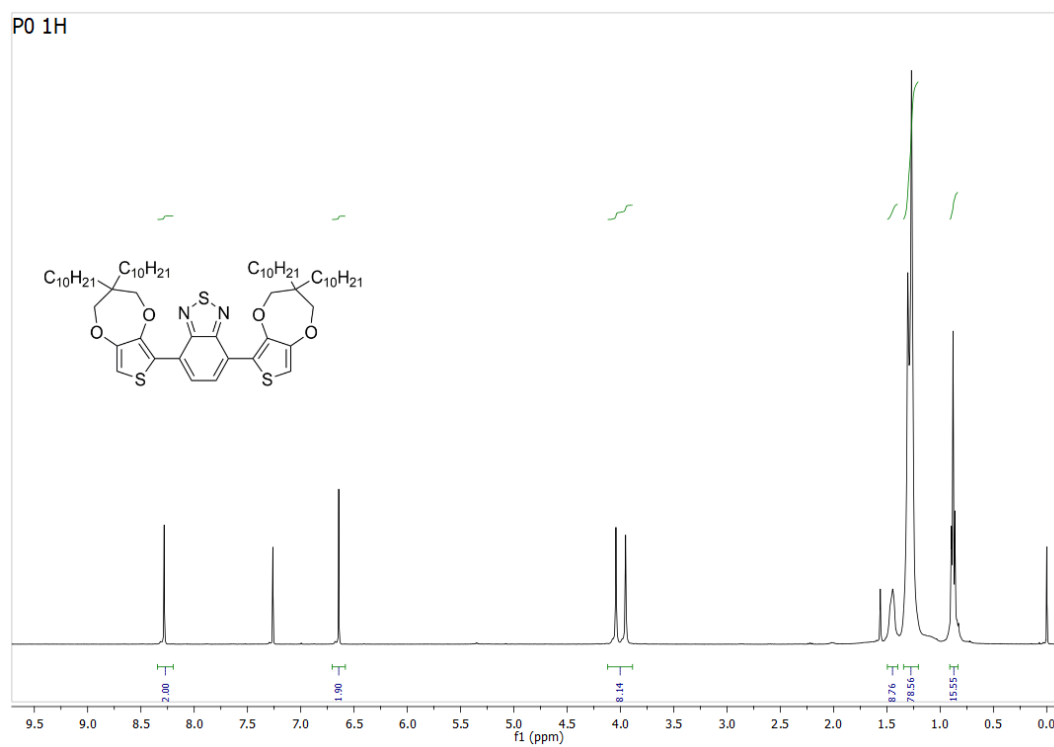
A. NMR Spectra of Monomers

Figure A.1 ^{1}H NMR Spectrum of **P0** in CDCl$_3$

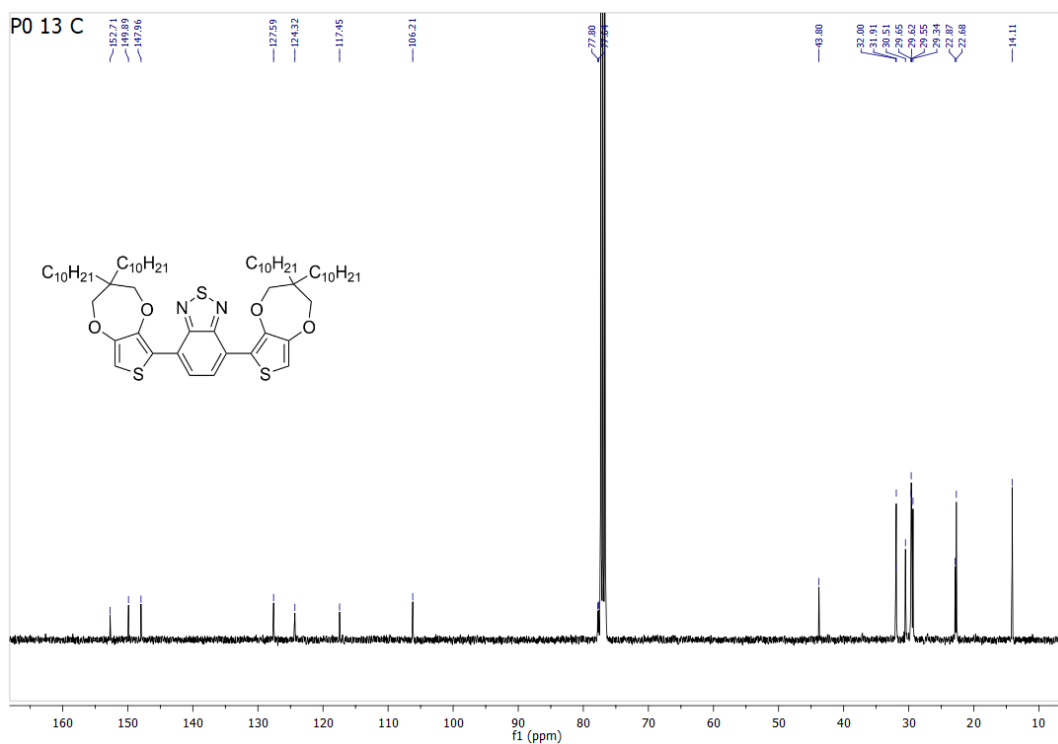Figure A.2 ^{13}C NMR Spectrum of **P0** in CDCl$_3$

P1 1H
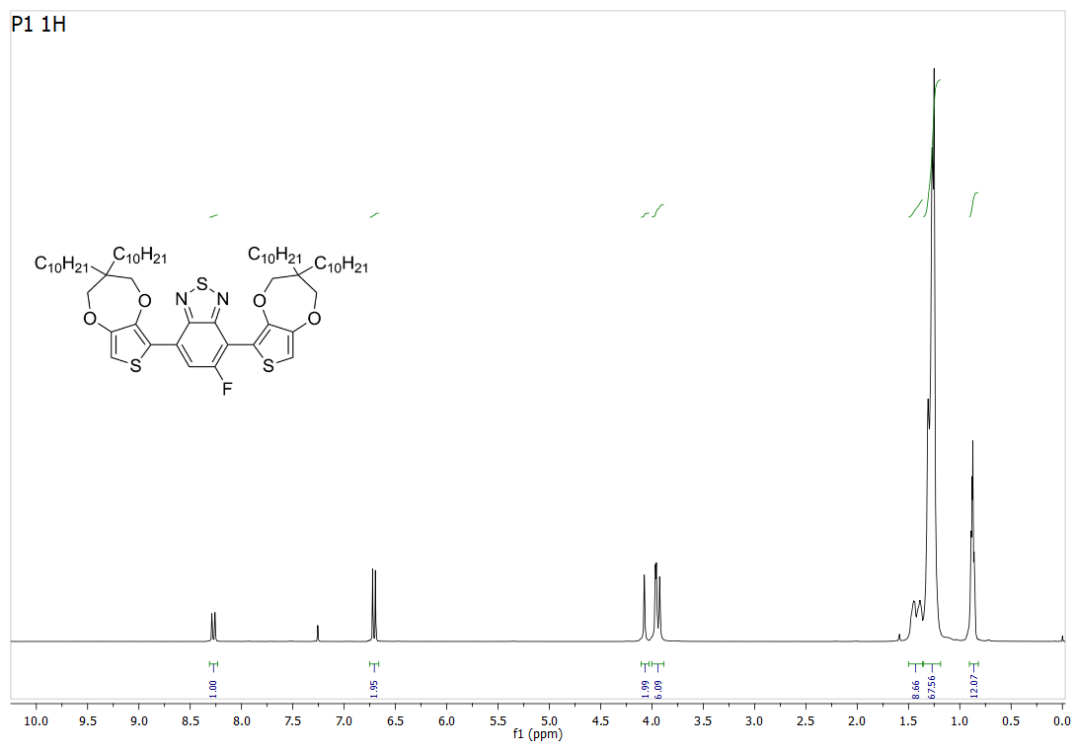

Figure A.3 ^{1}H NMR Spectrum of **P1** in CDCl$_3$
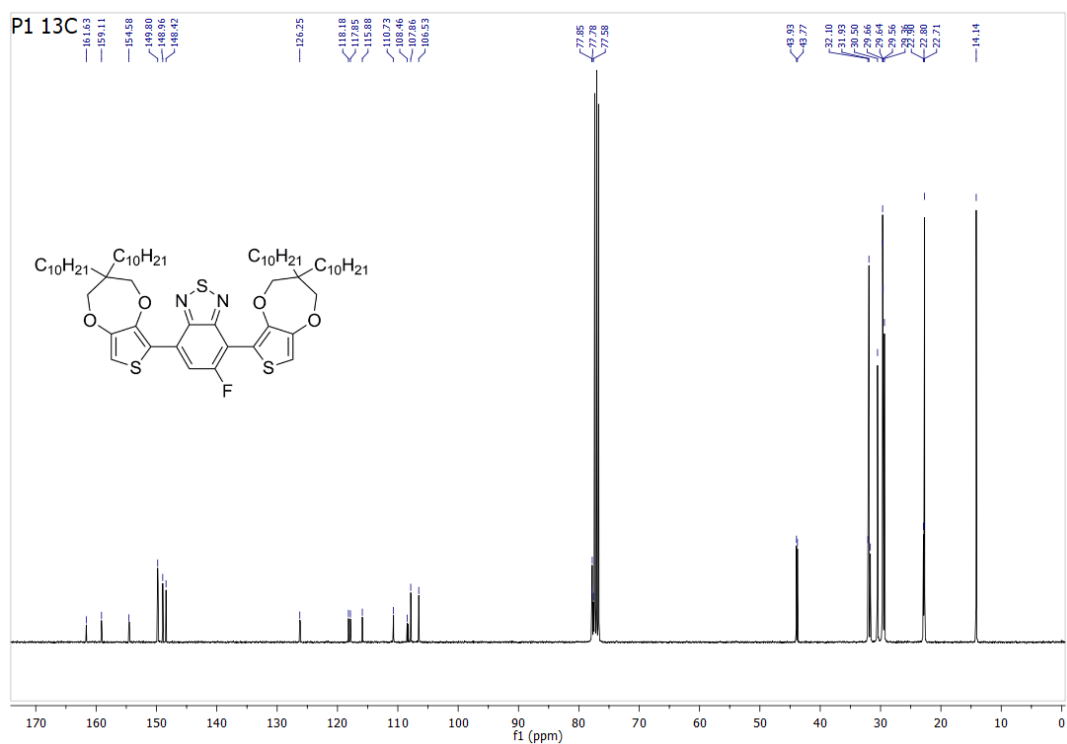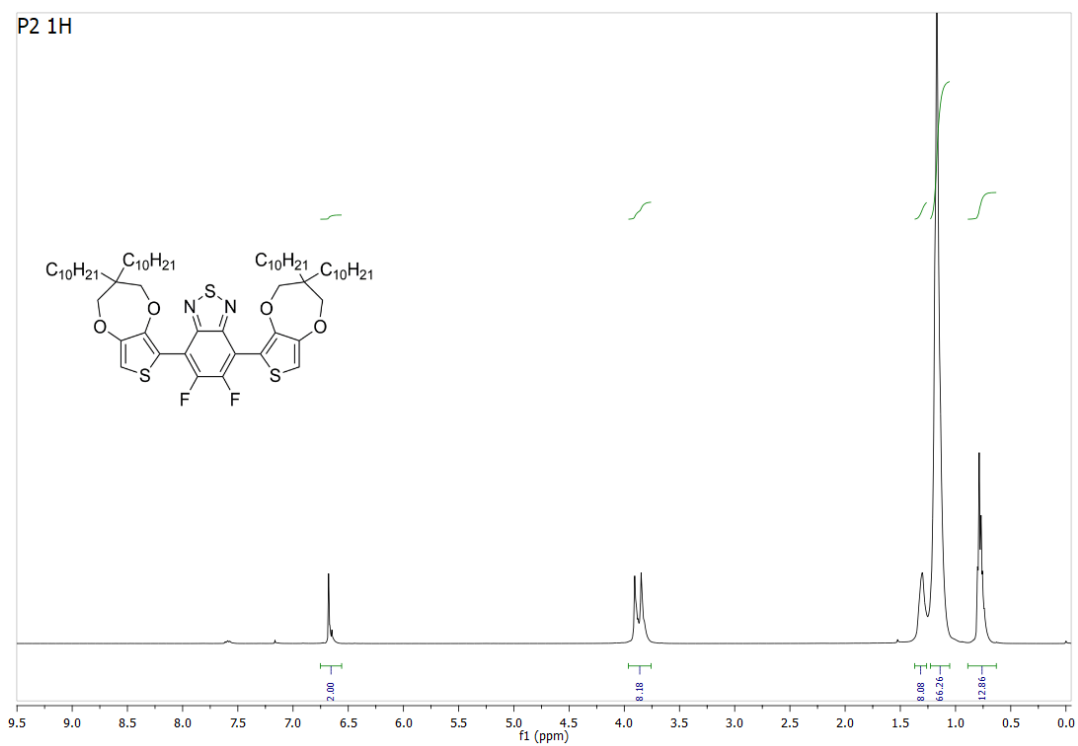
Figure A.4 ^{13}C NMR Spectrum of **P1** in CDCl$_3$
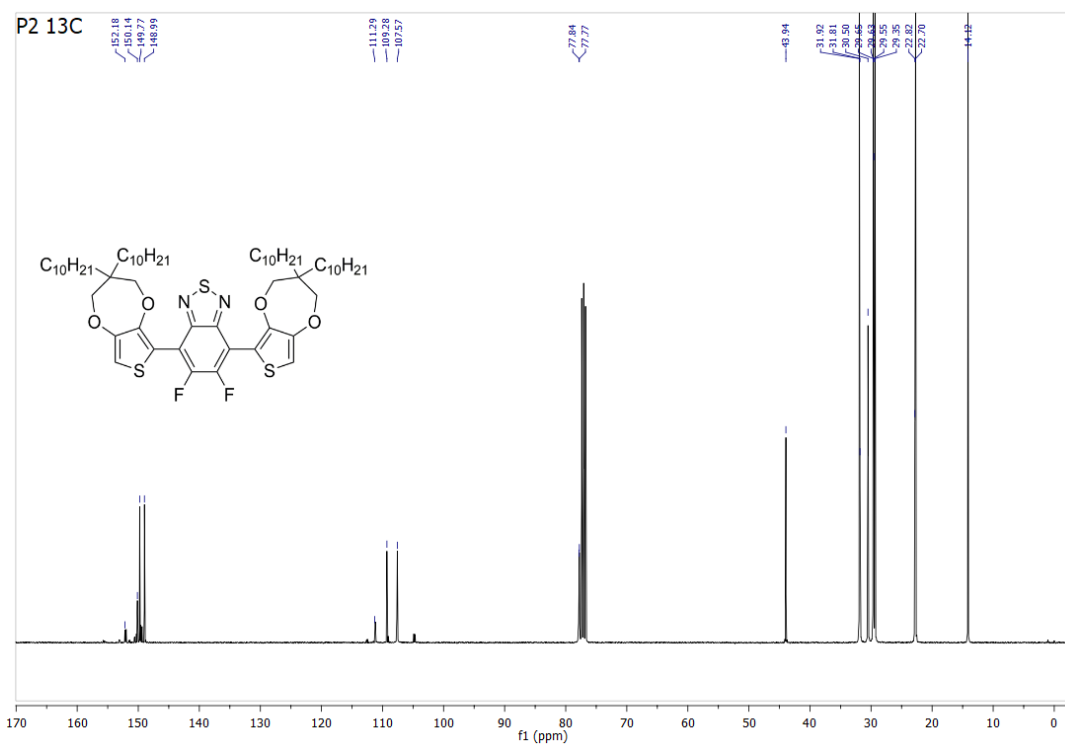
Figure A.5 ^{1}H NMR Spectrum of **P2** in CDCl$_3$

Figure A.6 ^{13}C NMR Spectrum of **P2** in CDCl$_3$
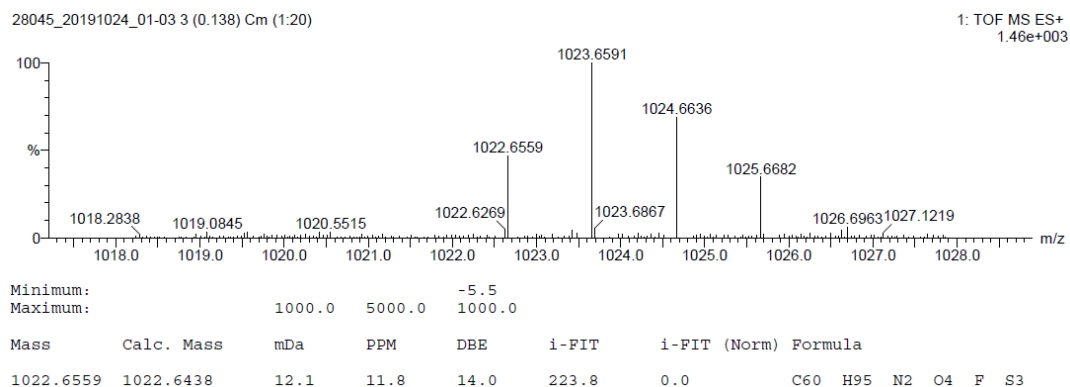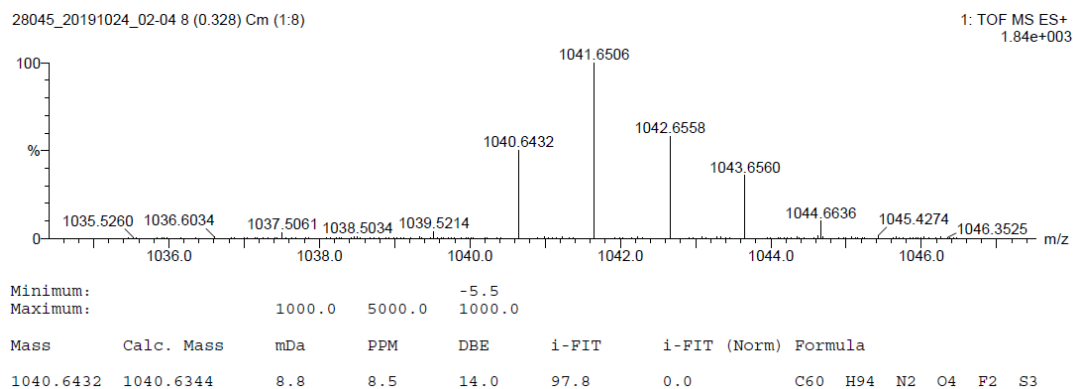
B. HRMS Spectra of Monomers

Figure B.1 HRMS Spectrum of **P1**

Figure B.2 HRMS Spectrum of **P2**